

Kaunas University of Technology
Faculty of Electrical and Electronics Engineering

Accuracy Assessment of a Computed Tomography based Reverse Engineering

Master's Final Degree Project

Apoorva Devaraj

Project author

Prof. Dr. Elena Jasiuniene

Supervisor

Kaunas, 2020



Kaunas University of Technology
Faculty of Electrical and Electronics Engineering

Accuracy Assessment of a Computed Tomography based Reverse Engineering

Master's Final Degree Project
Electronics Engineering (6211EX012)

Apoorva Devaraj

Project author

Prof. Dr. Elena Jasiuniene

Supervisor

Prof. Dr. Liudas Mažeika

Reviewer

Kaunas, 2020



Kaunas University of Technology
Faculty of Electrical and Electronics Engineering
Apoorva Devaraj

Accuracy Assessment of a Computed Tomography based Reverse Engineering

Declaration of Academic Integrity

I confirm that the final project of mine, Apoorva Devaraj, on the topic „Accuracy assessment of a computed tomography based reverse engineering“ is written completely by myself; all the provided data and research results are correct and have been obtained honestly. None of the parts of this thesis have been plagiarised from any printed, Internet-based or otherwise recorded sources. All direct and indirect quotations from external resources are indicated in the list of references. No monetary funds (unless required by Law) have been paid to anyone for any contribution to this project.

I fully and completely understand that any discovery of any manifestations/case/facts of dishonesty inevitably results in me incurring a penalty according to the procedure(s) effective at Kaunas University of Technology.

Apoorva Devaraj

(name and surname filled in by hand)

(signature)

Devaraj, Apoorva. Accuracy Assessment of a Computed Tomography based Reverse Engineering. Master's Final Degree Project/ supervisor Prof. Dr. Elena Jasiuniene; Faculty of Electrical and Electronics Engineering, Kaunas University of Technology.

Study field and area (study field group): Electronics Engineering, Engineering Sciences.

Keywords: X-ray Computed tomography, Reverse engineering, VGStudio max, MATLAB, Surface determination, Thresholding, Gray-value distribution and CAD.

Kaunas, 2020. 60p.

Summary

The presented work tells how accurate the reverse engineering process can be using x-ray computed tomography approach. Samples of different shapes and different materials were considered for investigation. The CT data was obtained with different sets of parameters to analyze which parameter set would give the accurate and best result of the reverse engineering process. The CT data were imported into VGStudio max, firstly surface of the object was determined after which all other processes like gray scale analysis, measurement analysis, mesh conversion and CAD conversion were carried out. The quality of CT data was best suited for investigation which was observed in gray scale distribution curves. The measurement analysis gave almost 98-99% accurate results and provided advantageous results using XCT than CMM approach. From the overall experiment, the results of the measurement analysis were almost 99% accurate and the gray scale analysis also gave flat curves indicating the absence of noise. This makes the overall accuracy of the x-ray computed tomography approach for the process of reverse engineering to be 98-99% on an average.

Devaraj, Apoorva. Kompiuterine tomografija paremtos atvirkštinės inžinerijos tikslumo įvertinimas Magistro baigiamasis projektas / vadovė Prof. Dr. Elena Jasiuniene; Kauno technologijos universitetas, Elektros ir elektronikos fakultetas.

Studijų kryptis ir sritis (studijų krypčių grupė): Elektronikos inžinerija, Inžinerijos mokslai.

Reikšminiai žodžiai: Kompiuterinė tomografija, atvirkštinė inžinerija, VGStudio max, MATLAB

Kaunas, 2020. 60p.

Santrauka

Pateikto darbo tikslas buvo įvertinti kompiuterine tomografija paremtos atvirkštinės inžinerijos tikslumą. Tyrimui buvo paimti skirtingų formų ir skirtingų medžiagų pavyzdžiai. Kompiuterinės tomografijos duomenys buvo gauti su skirtingais parametru rinkiniais, norint išanalizuoti, kuris parametru rinkinys duoda tiksliausią ir geriausią atvirkštinio inžinerijos proceso rezultatą. Pirmasis neapibrėžtumo šaltinis yra rentgeno spindulių parametrai, tokie kaip įtampa, srovė, vokselio dydis, didinimas ir kt. Atstumas tarp šaltinio ir objekto taip pat yra vienas iš neapibrėžtumo šaltinių. darbe buvo naudojamas kūginis rentgeno spindulių skenavimą, taigi, jei objektas yra arti šaltinio, kompiuterinės tomografijos vaizduose artefaktų galimybės yra didesnės. Kompiuterinės tomografijos duomenys buvo importuoti į „VGStudio max“ kur pirmiausia buvo nustatytas objekto paviršius. Buvo atlikti tokie tyrimai, kaip pilkumo lygių pasiskirstymo analizė buvo atlikta naudojant „VGStudio max“ ir sukurtą analizei programą MATLAB. Buvo nustatyta kad rentgeno kompiuterinės tomografijos metodo bendras tikslumas atvirkštinės inžinerijos procese yra 98–99%.

Table of Contents

List of Figures	8
List of Tables	10
Introduction	11
1. Survey On Reverse Engineering and it's application	12
1.1. Reverse engineering	12
1.2. Applications of reverse engineering in various fields	14
2. X-Ray Computed Tomography (XCT)	19
2.1. Principle of XCT	19
2.2. XCT parameters	20
2.3. Factors that cause artifacts in computed tomography	20
2.3.1. Beam Hardening.....	20
2.3.2. Cone beam error.....	22
2.3.3. Geometrical misalignments that leads to errors.....	23
2.4. Need for accuracy assessment	24
3. Methodology.....	25
3.1. Data Acquisition.....	25
3.2. Reconstruction	26
3.2.1. Thresholding	26
3.3. Image Processing	27
3.3.1. Surface determination.....	27
3.3.2. Measuring the samples	28
3.3.3. Gray scale analysis	29
3.3.4. Mesh conversion	30
3.4. Conversion to 3D CAD model.....	31
3.5. Accuracy assessment	31
4. Experimental investigations	33
4.1. Samples used for the experiment	33
4.2. X-ray parameters.....	34
4.3. Surface determination.....	35
4.4. Gray scale analysis	36
4.4.1. Gray scale analysis of Sample2	36
4.4.2. Gray scale analysis of sample3	38
4.4.3. Gray scale analysis of sample4	41

4.5.	Measurement of the sample	43
4.5.1.	Measurement results.....	46
4.6.	Mesh conversion	52
4.7.	Conversion of 3D CAD model	55
	Conclusion	57
	References	58
	Appendices	60
Appendix 1.	The International Young Scientists Conference “Industrial Engineering 2019” on topic “Assessment of Factors Influencing Accuracy in a Computed Tomography based Reverse Engineering”	60

List of Figures

Figure 1.1. Reverse engineering process[5]	12
Figure 1.2. RE aided remanufacturing framework for worn components or parts[10]	15
Figure 1.3. Point cloud view after 3D scanning process[11]	16
Figure 1.4. (a) Modeled part of front fender (b) Assembly view[11].....	17
Figure 2.1. A cone beam XCT system's schematic[14].....	19
Figure 2.2. The scanned image showing beam hardening effect and its intensity profile[14]	21
Figure 2.3. The scanned image showing reduced beam hardening effect using copper film and its intensity profile[14]	21
Figure 2.4. The scanned image showing reduced beam hardening effect using software and its intensity profile[14]	21
Figure 2.5. Image of the sample and the CT image with artifacts due to cone beam error[14]	22
Figure 2.6. Incident angle and the horizontal axis with respect to detector[14].....	22
Figure 2.7. Perfectly aligned CT system schematic representation[15].....	23
Figure 2.8. Detector angular misalignment[15].....	23
Figure 3.1. The flow graph of the accuracy assessment of a computed tomography based reverse engineering.	25
Figure 3.2. Computed tomography experiment setup.....	25
Figure 3.3. Histogram of a CT image	27
Figure 3.4. Fitting of cylinders to measure the outer and inner diameters.....	28
Figure 3.5. Planes fitted in the middle of each step	29
Figure 3.6. Gray scale analysis performed in VGStudio max	29
Figure 3.7. gray scale analysis performed in MATLAB.....	30
Figure 3.8. Point reduction process[18]	31
Figure 3.9. Mesh simplification[18]	31
Figure 4.1. Sample1-Plexiglass cylinder with dimensions.....	33
Figure 4.2. Sample2-Plexiglass cylinder with holes and its measurements	33
Figure 4.3. Step cylinder with dimensions	34
Figure 4.4. The surface determined CT image	36
Figure 4.5. 3D view of gray value density distribution of a part of 5 mm from the top surface where (a) sample2 scanned using scan1 parameters and (b) sample2 scanned using parameters of scan2	36
Figure 4.6. 2D view of gray value density distribution of a part of 5 mm from the top surface where (a) sample2 scanned using scan1 parameters and (b) sample2 scanned using parameters of scan2	37
Figure 4.7. The gray scale image showing the line across which the gray value distribution is plotted.....	37
Figure 4.8. The gray value distribution plot of pre-defined line of scan1 and scan2 respectively ...	38
Figure 4.9. CT image showing the predefined line.....	38
Figure 4.10. Gray scale distribution for the first parameter set with magnification_1.25	39
Figure 4.11. Gray scale distribution for the parameter sets with magnification_2.....	39
Figure 4.12. Gray scale distribution for the parameter sets with magnification_2.5.....	40
Figure 4.13. Gray scale distribution for the parameter sets with magnification_5.....	40
Figure 4.14. CT image of aluminum step cylinder showing the pre-defined line	41
Figure 4.15. Gray scale distribution for the parameter sets with magnification_2.5	41

Figure 4.16. Gray scale distribution for the parameter sets with magnification_5	42
Figure 4.17. CT image of step cylinder showing the pre-defined lines	42
Figure 4.18. Gray scale distribution at each step of the step cylinder	43
Figure 4.19. CT images of sample1. (a) 3D view (c) Front view	43
Figure 4.20. CT images of sample2 with noise (a) 3D view (b) Right view	43
Figure 4.21. CT images of sample2 with reduced noise (a) 3D view (b) Right view	44
Figure 4.22. CT images of sample3 without noise (a) Right view (b) 3D view.....	45
Figure 4.23. CT images of sample3 with noise (a) Right view (b) 3D view	45
Figure 4.24. CT images of sample4 (a) Right view (b) 3D view	45
Figure 4.25. Plots of measurements v/s deviation of sample2	47
Figure 4.26. Plots of diameters v/s its deviation of sample3 according to the magnification factor	48
Figure 4.27. Diameter v/s its deviation curves with different magnification value.....	49
Figure 4.28. Hole diameter at each step with respect to outside step diameters	50
Figure 4.29. Plots of diameters v/s its deviation of sample4 according to the magnification factor	51
Figure 4.30. Diameter v/s its deviation curves with different magnification value.....	52
Figure 4.31. Meshed images of scan1 parameter set of sample2. (a) 3D view (b) Front view (c) Right view	53
Figure 4.32. Meshed images of scan2 parameter set of sample2. (a) 3D view (b) Right view.....	54
Figure 4.33. Meshed CT images of step cylinder of plexiglass step cylinder	54
Figure 4.34. Improper meshed CT images of step cylinder of scan8 parameter set of plexiglass step cylinder.....	54
Figure 4.35. Meshed CT images of scan8 parameter set of plexiglass step cylinder	55
Figure 4.36. Meshed CT images of step cylinder of aluminum step cylinder.....	55
Figure 4.37. Mesh file converted to CAD file	56

List of Tables

Table 1.1. Comparison between CMM technique and CT technique for data Acquisition[6]	13
Table 5.1. XCT scanning parameters used for sample1 and sample2.....	34
Table 5.2. XCT scanning parameters used for plexiglass step cylinder (sample3)	35
Table 5.3. XCT scanning parameters used for aluminum step cylinder (sample3)	35
Table 5.4. Iterations of surface determination with automatic and advanced settings.....	44
Table 5.5. Measurement results of Sample2.....	46
Table 5.6. Measurements of step cylinder for different CT scan data	47
Table 5.8. Measurements of the diameter of the hole at each step of step cylinder for different CT data.....	50
Table 5.9. Measurements of the aluminum step cylinder.....	51
Table 5.10. Iterations of Mesh conversion process.....	53

Introduction

Reverse engineering is a process used to reproduce the whole geometry or a part of an available physical object. Reverse engineering is used to duplicate parts and also the part drawing prints from many decades which are used in military, defense sectors etc. There are many different approaches for implementation of reverse engineering which are presented in scientific literature. Most of the approaches are based on point cloud analyses which are acquired through coordinate measuring devices like, Coordinate Measuring Machines (CMM), optical scanners or interferometric systems. CMM and CAD/CAM software like Mastercam, ProEngineer etc are used in duplicating the parts. The mechanical objects are usually digitized using CMM[1].

Computed tomography (CT) is a procedure of x-ray imaging of an object which is computerized. The CT technology has improved rapidly in industrial applications in the recent years. One among them is the nondestructive testing (NDT). Using CT for the process of reverse engineering is advantageous as it captures the internal structure without much effort as in other approaches like CMM, which requires segmenting the object or placing the object at different positions to obtain particular part of the object[2]. In most cases, obtaining the internal structure of the object is only possible using the CT.

Reverse engineering process approach using CT has still a long way to go, as the advantages of using CT in industrial applications is coming to light with wide variety of use in the recent years. To prove that the CT is one among the best and easier approach for the reverse engineering process, finding the accuracy of the process becomes important. There are many uncertainties that can hinder the accuracy of the process. To find the factors that influence the accuracy throughout the reverse engineering process is another challenge. The factors like the x-ray parameters used during the CT scan, threshold value for reconstruction, parameters for surface determination etc, can influence the accuracy of this process. Correcting these factors to obtain the accurate results of the reverse engineering process using CT approach is the next task that follows after finding the accuracy influencing factors. For measurement analysis the CT approach gives better results, because even the internal structure of the object is obtained without literally slicing the object.

The main objective of this investigation was to determine the accuracy of the computed tomography based reverse engineering and the sources of uncertainties that influence the accuracy. The steps to be followed to achieve the objective of the investigation are

- Literature review of the previous related works on reverse engineering and its applications.
- Determination of steps of reverse engineering process.
- Determination of factors influencing the accuracy of CT based reversed engineering.
- Determination of optimized CT investigation parameters to obtain accurate results.
- Finding the final accuracy of the reverse engineered model by comparing it with the initially designed model.

1. Survey On Reverse Engineering and it's application

1.1. Reverse engineering

Reverse engineering is a process in which the object under investigation is examined to obtain the complete understanding of its assembly, construction and also its functionality. Reverse engineering is widely used nowadays for industrial designs, cloning, duplication and also reproduction[3]. Reverse engineering originally was defined as “the process of developing a set of specifications for a complex hardware system by an orderly examination of specimens of that system” and also Chikofsky and Cross defined it as “the process of analyzing a subject system to identify the systems components and their relationships, and to create representations of the system in another form or at a higher level of abstraction”. In literature reverse engineering is generally addressed from different perspectives which include benchmarking of the system and its recovery, and inverse problem modeling to obtain the model and parameters of the model from the experimental data.

Considering the geometrical aspect of the product have led to high growth in research of geometrical reverse engineering or reverse geometric modeling. Reverse engineering of a geometric model is normally based on an approach which involves geometry of the given product is extracted which is then used to reconstruct a 3D model[4]. The whole of reverse engineering process can be explained in three basic steps: product or the sample digitization, shape reconstruction and 3D CAD modelling, the process flow is shown in figure (1.1)[5].

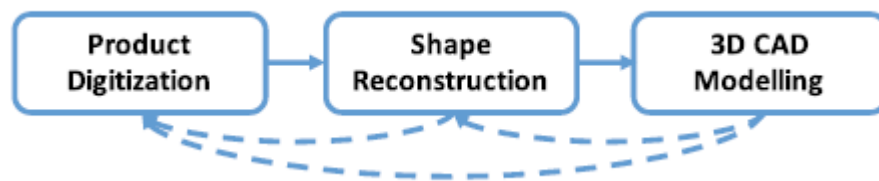


Figure 1.1. Reverse engineering process[5]

The first step is product digitization, which in general refers to digitizing the physical object using the scanning devices or measuring devices. This step or the phase includes many processes like mechanical simulation, manufacturing process simulation and shape and topology optimization. This phase of product digitizing is used for integration of material properties, manufacturing processes and also their inherent variability[5].

The second step is reconstruction of the physical object which is to determine a surface that is approximately same as the unknown shape of the object or the sample. The digitized data set can be characterized into variable density due to the noise and the outliers which occur because of the acquisition process. The main criteria for the reconstruction process is to make sure that the original topology of the object is preserved and the sharp features and surface boundaries can be reproduced accurately on the reconstructed surface. The literature for the techniques used for this purpose is vast. The previously used techniques like NURBS or B-splines which were used to fit together the local surface patches had their limitations when working on complex physical objects or large data or the noise and also they were not applicable when physical properties like the material used or density of the object were involved[5].

The final step to create the geometric product of the sample is the 3D CAD modeling using the boundary representation or a feature based representation that embed the design with the geometric features, parameters and the constraints. For the purpose of design modification or for model query and interrogation, feature based parametric models are required. These parametric models develop knowledge based reverse engineering approaches for inclusion of priority information to obtain more design and manufacturing data by overcoming noisy data or missing data[5].

Reverse engineering has a long way, where it was performed only using scanning devices or the measuring machines. Using CT for the purpose of reverse engineering is still new in industrial field. The geometrical features are measured using the CT generated 3D datasets which is similar to the traditional coordinate measuring machines (CMM) or the visual measurement machines (VMM) which are now realized by the industries[6].

Table 1.1. Comparison between CMM technique and CT technique for data Acquisition[6]

	CMM	CT
Measurement strategy and preparation	The features of interest are to be known by. The operator has to know how to reach these features and to mount the sample accordingly. The sample has to be cut into parts sometimes to reach the interested feature or the region of the sample or the sample or the part of interest has to be placed in different positions. For accurate measurements the probe's physics (length, diameter) has to be known.	The major task involves placing the sample on the turntable while avoiding long material paths, which causes lack of penetration, and also to avoid critical planes along the beam, which causes partial volume effect.
Program setup	The features of interest have to be programmed. The operator must ensure that the features to be measured are reachable to the probe and also should be able to decide the points to be used as well as the angle at which the probe touches the surface. The probe force might also be considered which may be critical in some applications.	The main focus of the approach is to obtain data that measures the features of the sample. Considerations at this step are the number of projections, integration time, voltage and current and also saturation levels of the detector which can be time consuming.
Data Acquisition	The sample may need to be placed at different positions while the probe traces the path as set in the program. This leaves the operator to be present at all times repeating the steps of program setup and data acquisition.	If determination of x-ray parameters is done the sample is rotated on the turntable at 360 degrees to acquire the views hence the operator need not be present with the system.
Analysis	The protocol with all the measurement values is created by	After the data is acquired the strategy for the measuring the

	the software. It is required that the sample remains in the system for changes and even reprogramming may be necessary.	required feature is done by the operator. Even at the later stage changes in the strategy of measurement can be easily applied without measuring the part again.
Additional information	None	Internal defects are shown in full surface 3D model.
Limitations	Segmenting the sample for required feature measurement and internal features are the limitations.	Multi-material parts and large dense parts are the limitations.

The major reason for using the CT in place of old typical non-destructive optical and tactile methods is the ability to measure the unreachable and invisible features of the sample. CT measures the internal features of the object without even contacting the actual part or cutting into the object. Table (1.1) shows the comparison between CMM technique and CT technique with its advantages and disadvantages for data acquisition in industrial processes[6]. Using CMM for obtaining the data set for the process of reverse engineering gives good results but has its disadvantages; using CT may be a way to overcome these disadvantages. For obtaining the digital data of the object using CMM may require to segment the sample, which may sometimes result in malfunctioning of the sample or it may require scanning the same sample in different angles to obtain a certain complex part of the sample. All these may not be required in case of CT as it can measure the sample internally without contact.

1.2. Applications of reverse engineering in various fields

Reverse engineering is carried out in almost all the fields. It can be used in any field to extract the data of any material, product or system. It is very important in the field of additive manufacturing. Image based reverse engineering was used to visualize the prototyping of woven cloth[7]. Reverse Engineering can also be used to perform the morphological operation on a PCB using MATLAB. One of the most difficult and important step in the process of reverse engineering is image segmentation because it requires deep understanding of the image. The first step in the PCBs reverse engineering is to identify the components which are mounted, its interconnections between the layers, its pins and ports and many more[8].

Reverse engineering is a process using which, systems or objects are examined to obtain the information of the internal construction, assembly and functionality. RE was considered to be a destructive process which includes disassembling the systems and devices into several different parts which are then used in many fields such as industrial design, cloning, duplication and reproduction. The motivation to perform RE may be an honest one or a dishonest one. RE used for the purpose of verification, fault analysis, research and development, educating etc, about the workings of any existing product or system or to enhance the systems are all under honest motivation. The ones with dishonest intentions are to clone, pirate, counterfeit a design, to develop an attack, to insert a hardware Trojan[9].

In a PCB the components and the chips that are mounted on the silicon board which is non conductive and then are interconnected using electrically conductive copper traces. The functional complexity of the electronic device decides the layers of the PCB that is, single layered or multi-

layered. The PCB reverse engineering process starts with segregating the components of on the board, its interconnections or traces between the components of same layers or connection between the layers, its ports for external connection and so on. After these processes, de-layering is carried out in destructive RE and x-ray imaging is carried out in non-destructive RE to identify the connections, traces, and vias of the internal PCB layers[9].

The mechanical components or parts that are worn are remanufactured. To reduce the environmental effects the waste or deposited mechanical parts' remanufacturing is one of the emerging solution and it also reduces the financial expenditure by extending their lifespan. These worn mechanical parts that arrive for remanufacturing possess high variability of failures and also high structural complexity. The manual repair to restore the original shape is time consuming, labor intensive and also of low quality. Reverse engineering technologies as an aid, this process can be made automated for a quick and accurate acquisition of the area of damages and facilitating the further processes of remanufacturing. The below algorithm shown in figure (1.2) is the proposed algorithm for automated decision making of the processes to be carried out for remanufacturing of the worn parts. The approach includes 3D surface data collection, nominal model reconstruction, and fine registration, extraction of additive/subtractive repair, tool path generation and actual machining process. All these processes seek to improve the efficiency and reliability of the remanufactured parts[10].

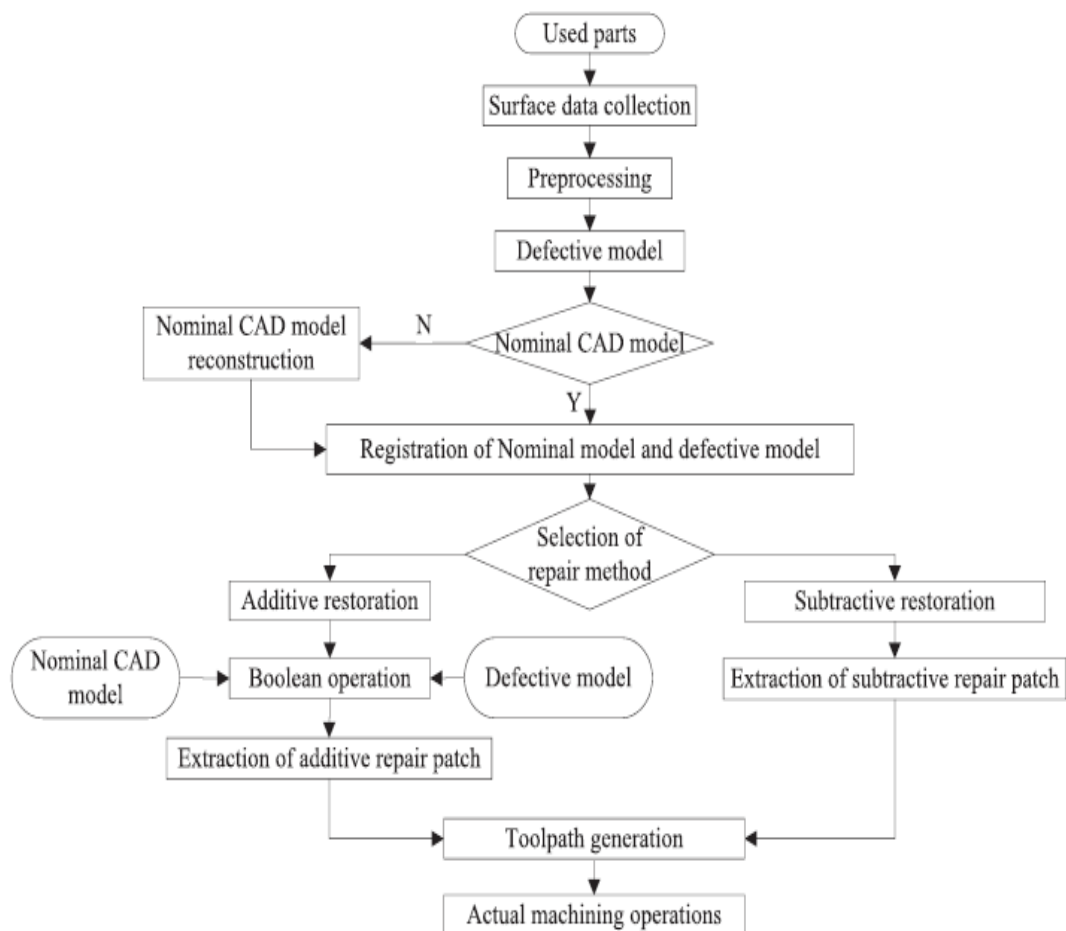


Figure 1.2. RE aided remanufacturing framework for worn components or parts[10]

The nominal model reconstruction uses a prominent cross section algorithm and a curvature constraint is adopted to automatically eliminate the defective point clouds in the damaged area of the worn parts. With this reconstructed nominal model and the 3D model, the registration process based on a modified ICP algorithm is carried out to eliminate the corresponding pairs of two models which are unreliable and hence give a best-fit position of two models. A proper repair strategy is determined on the basis of obtained registration results along with the extraction of the additive/subtractive repair patch. Through a CAD/CAM system such as CATIA software the tool paths for virtual repair process are generated. Later to drive the machine tools for an actual repair process numerical control codes are produced[10].

A method of transformation of a real life object into digital form was described and presented. A motorcycle front fender of scale 1:12 was investigated. After the CAD model and design of the product, it is submitted for production. By a proper set of characteristic properties, the design is described and also saved for the future use. Due to the complexity of some models the technical drawings becomes very complicated. These models can be realized by simply transferring the CAD models for 3D printing or to the CNC machines. 3D scanning technique consists of a high intensity light source and complex software cooperated along with the detector which is used to reconstruct the shape of the object. The scanned object is then converted into a triangle mesh or a point cloud as shown in figure (1.3). Based on this conversion the use of CAD tools further process of restoration of shape of the object is done. This process is called reverse engineering or back engineering[11].



Figure 1.3. Point cloud view after 3D scanning process[11]

The 3D scanning technique has a main disadvantage that is the part of data, details of an original element can be lost permanently, hence all these lost features should be recreated during the CAD designing. The investigated object is a tiny part with dimensions 1cm x 2cm x 3cm and with a thickness of 1mm. It should be noticed that this fender is a two symmetrical parts glued together. The modeled part of the fender and its assembled view is shown in figure (1.4) below[11].

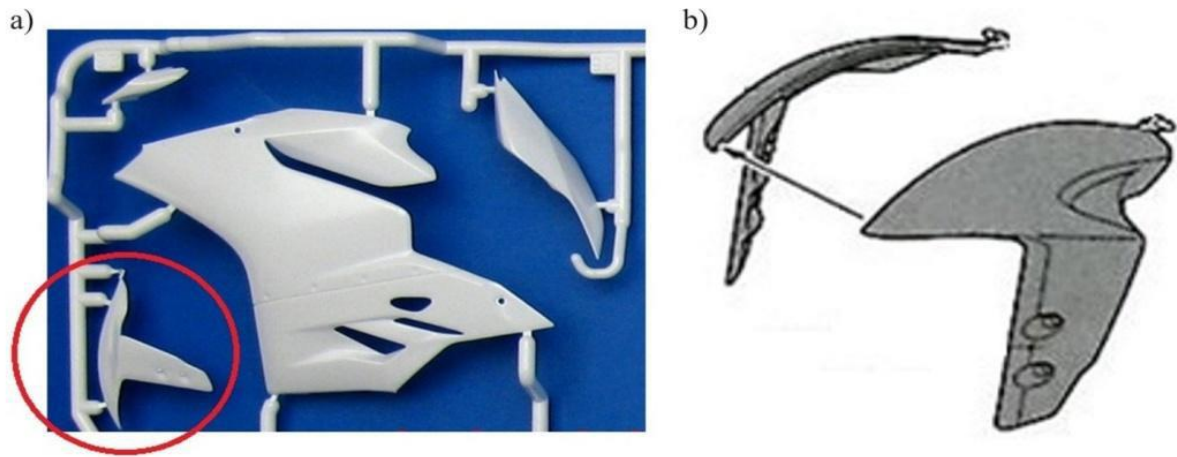


Figure 1.4.(a) Modeled part of front fender (b) Assembly view[11]

After cleaning of the cloud, as a next step these clouds are joined together by means of accurate positioning and three point positioning and finally these arranged clouds are merged together. On the basis of the chosen characteristics points from the point cloud the sharp curve is created. After the desired details are achieved in the model, it is 3D printed as it is the fastest and cheapest way to transform CAD models into real life objects. Later on it is painted and installed[11].

Turbine blades are meant to be one of the expensive mechanical parts. Even if all the possible activities of refurbishment are examined, nobody throws them away. The sample considered for the purpose of reverse engineering may also be refurbished parts that already possess some errors. A new approach was described that is used to process the data points that are measured from the turbine blade airfoils so that through reverse engineering a valid shape is obtained. Presently a preliminary B-rep model is created through fitting surfaces to point clouds using 3D laser scanner. Due to the high complexity of the turbine blades, a small change in its geometry can give large change in turbine performance. A new method using segmentation and constrained fitting algorithm is to be implemented for the process of reverse engineering to obtain high performance results. Another way to define reverse engineering might be involved in deducing the intent of the original design[12].

Reverse engineering might be bounded in case of the quality of measurement and the complementary computer aided modeling activities. Few other limitations of the reverse engineering are:

- Sensing errors – Errors that occur during data acquisition stage can be reduced by improving the sensing techniques' precision. Yet some amount tolerance is present in any measurement.
- Approximation errors – The assumptions that are made about the data set depending on the chosen method for reconstruction influences the way in which the data is approximated.
- Numerical error – During the process of reconstruction noise is introduced in numerical ways and can be avoided by using stable method, but cannot be avoided as long as computing with floating point numbers.
- Wear of the object – Any mechanical objects' external surface is subjected to wear. Hence even when measurement errors are avoided there is limited access to correct the geometry.

The new algorithm can be a general method of reverse engineering and not limited to any special type of application. This can be used as a substitute some of the knowledge about the geometric construction of a part. The whole section geometry of the turbine blades are managed by constrained fitting. The SCFA algorithm implemented on turbine blades show results with successful filtered profile[12].

Producing digital model of mechanical parts using measured data points is one of the important areas of reverse engineering. The numerical algorithms such as aligning point clouds, mesh processing, surface fitting and segmentation that are used for the process of reverse engineering may give rise to errors and also the addition of noise adds to the inaccuracies. As a result of these inaccuracies, smooth connections may be of poor quality, faces may not be precisely parallel or orthogonal, and axes of concentric cylinders may be slightly tilted and so on. To eliminate these uncertainties and create perfected B-rep model the algorithms are described[13].

Reverse engineering technology is widely utilized in different applications where an object is scanned in 3D and the computer represented object is under gone various computations. A crucial issue in the technique of reverse engineering is that the perfection of objects that was reconstructed from the measured data. The hypothetical local and global constraints are detected in this approach which numerically qualifies as relevant surfaces to be kept for computing best-fit structures by related constraints[13].

2. X-Ray Computed Tomography (XCT)

2.1. Principle of XCT

X-ray computed tomography (CT) is one of the growing non-contact measuring techniques in industrial applications. It performs wide variety of dimensional and geometrical measurements. Compared to the traditional tactile and optical coordinate measuring machines CT offers many advantages as it provides holistic measurements of the scanned objects. CT provides high potential in quality control in the rapidly developing additive manufacturing techniques that are capable of producing highly complex parts with non-accessible geometries. It can visualize in three dimensions both external and internal structural parts and it can also detect defects without contact or damaging the investigated part. It has the potential to carry out dimensional measurements at micrometer level[14].

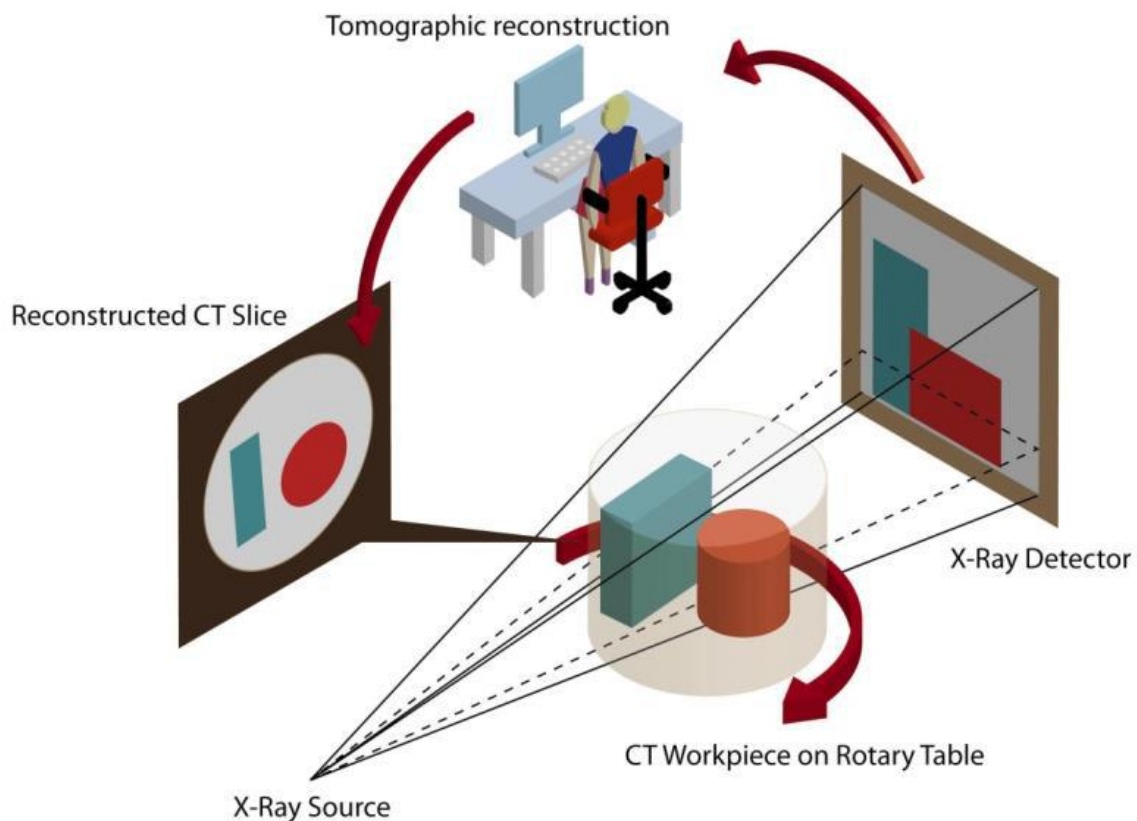


Figure 2.1. A cone beam XCT system's schematic[14]

An x-ray computed tomography system consists of an x-ray source, a sample manipulating system, radiation detector and a computer system to analyze it. The above figure (2.1) shows the schematic view of a cone beam x-ray computed tomography system used in industries. The object is placed on the rotary table that rotates according to the parameters set so that the whole object is scanned. These parameters are set using the manipulating system according to the requirement of the investigation[14].

The XCT system uses x-ray as the source to take multiple two dimensional transmission images of the object to be investigated in different orientations so as to cover the whole object. These 2D images are then reconstructed to form a 3D volumetric data set of the scanned object and thus the

surface can be extracted from the volumetric data. Due to the improvement in the x-ray sources, detectors and computing techniques, XCT is now been widely used for scanning different objects from composites to metals. These advances have taken XCT to be extensively used in industrial applications. The cone beam computed tomography utilizes the two dimensional detector that allows to scan the entire object in a single rotation as compared to conventional CT scanners whose 2D slices had to be stacked to obtain a complete image. Cone beam technology is more efficient as it uses x-rays efficiently and requires less electric energy[14].

2.2. XCT parameters

All the x-ray parameters are operated from the x-ray operating room. To scan an object there are many parameters to be set voltage, current, voxel size, focus size, magnification, average time for the scan, number of projections, distance from the source or the detector etc. Each of these parameters can affect the CT data. Selecting these parameters in an optimized way is a great challenge. If high voltage is given, it results in too bright images which give error during the surface determination and low voltage reduces the penetration power of the x-ray beam. A high voxel size value gives high signal to noise ratio but with a trade off for low spatial resolution. The distance of the object from the source or the detector has to be selected in a moderate way as the x-ray scan uses the cone-beam x-ray technique which results in too large incident angle when the object is placed near to source, this results in improper scanning of the object like the edges or the surface of the object may be cut-off. Few examples of the artifacts that may occur in the CT data are given in below sections.

2.3. Factors that cause artifacts in computed tomography

CT systems one of the important requirement is the study of measurement accuracy and traceability to the unit of length. The CT measurements are affected by a number of quantities that influence the accuracy like scanning parameters, sample material and size, geometrical misalignments etc. XCT has many advantages but because of the systematic errors and their impact on dimensional analysis its usage is hindered. Some of the errors that influence the CT measurements are beam hardening, cone beam error, misalignments, under-sampling, truncation, ring artifacts, metal artifacts and noise artifacts.

2.3.1. Beam Hardening

Beam hardening is a phenomenon that is attached with the computed tomography system using polychromatic x-ray source that composes of photons of multiple energies. As the x-ray travel through the x-ray absorbent material or the object the lower energies are attenuated than the higher energies, this increases the average x-ray energy. But the reconstruction algorithm works on an assumption that the attenuation is the only property of the material and does not depend on the energy of the x-ray photon. This assumption and reality mismatch leads to errors in estimating the attenuation coefficient of the material and creates artifacts in the image known as cupping where the object is brighter at the edges and darker at the centre[14].

A steel sphere was considered as the sample for investigation in article. The below figure (2.2) shows the effect of the beam hardening error where the steel sphere is been scanned by cone beam XCT system the intensity variation across the sample which is contradictory to the homogenous

material property is shown in the cross sectional image with the gray value intensity profile across the centre of the image[14].

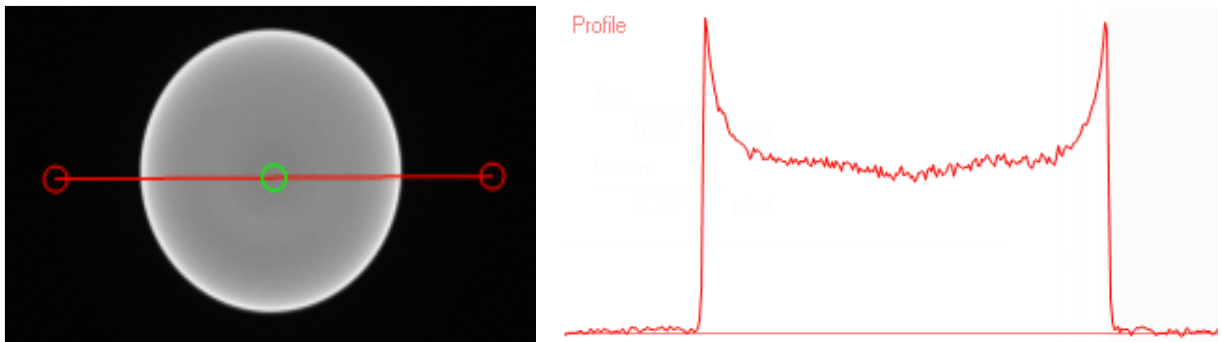


Figure 2.2. The scanned image showing beam hardening effect and its intensity profile[14]

There are two ways commonly used to reduce the beam hardening errors. The physical correction is one way that uses an additional component like a copper film. This added copper film attenuates the lower energy photons of the x-ray beam such that the beam hardening effect is less significant on the object under examination. The figure (2.3) below shows the CT image of corrected beam hardening effect through copper film and its intensity profile. But this increases the current required to compensate the decreased number of photons that are propagating. Increasing the current may lead to reduced lifespan of the x-ray filament, increase in the focal spot size and consequently reduction in the resolution of the scan.

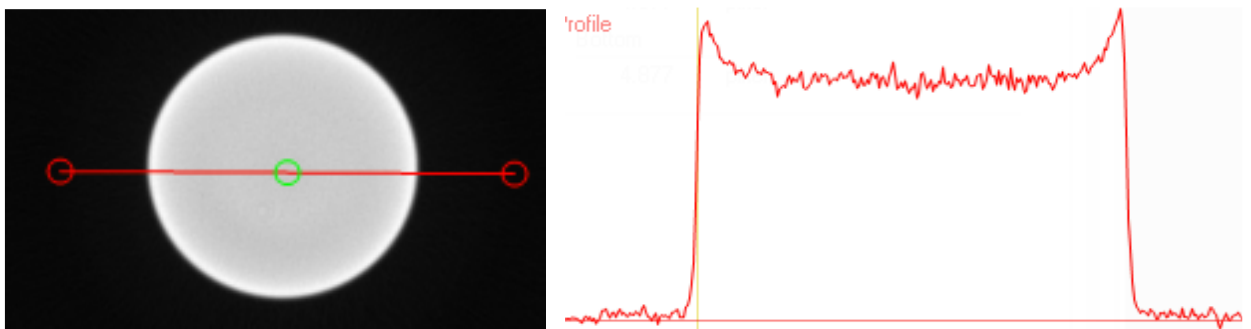


Figure 2.3. The scanned image showing reduced beam hardening effect using copper film and its intensity profile[14]

Another way apart from the physical filtering is by numerical corrections through software. The figure below (2.4) shows the software corrected CT image and its intensity profile.

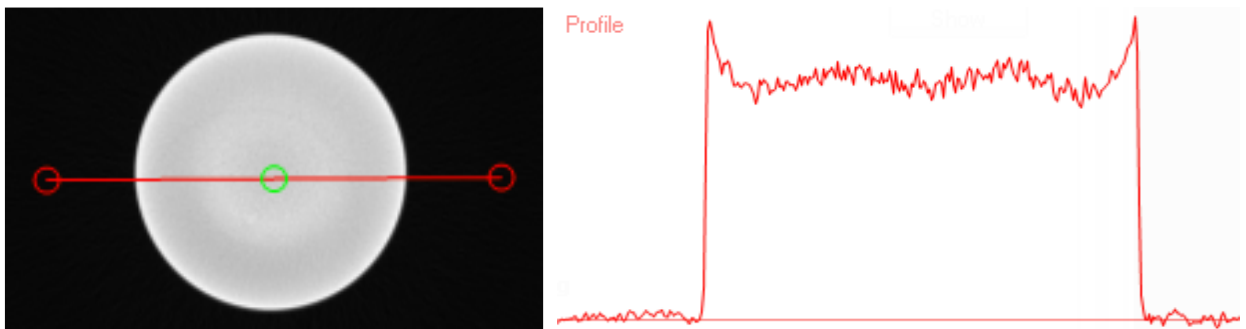


Figure 2.4. The scanned image showing reduced beam hardening effect using software and its intensity profile[14]

The beam hardening effect is even more complicated on the complex sample measurements such as the additive manufacturing samples. This error can be reduced using different preset numerical corrections. A lower index preset algorithm shows better reduction in the beam hardening error than the higher index algorithms but there is no quantitative evaluation to support regarding the optimum preset algorithm.

2.3.2. Cone beam error

Many cone beam XCT systems with flat detectors for reconstruction of scanned images use algorithms developed by Feldkamp as it is highly efficient in computing compared to other reconstruction algorithms. But this algorithm works on the assumption that at the trajectory of the source is circular which produces artifacts. Many improvement works are carried out for this reconstruction algorithm[14].

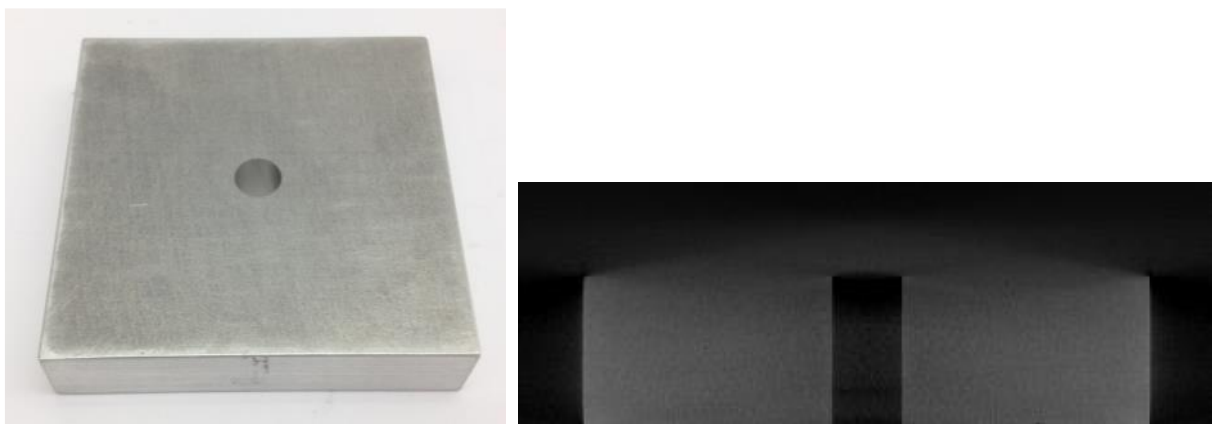


Figure 2.5. Image of the sample and the CT image with artifacts due to cone beam error[14]

The above image (2.5) shows an example of an image that contains artifacts, this happens when the incident angle of the x-ray beam with respect to the object is not optimized. The incident angle and the horizontal axis with respect to the detector is shown in the below figure (2.6).

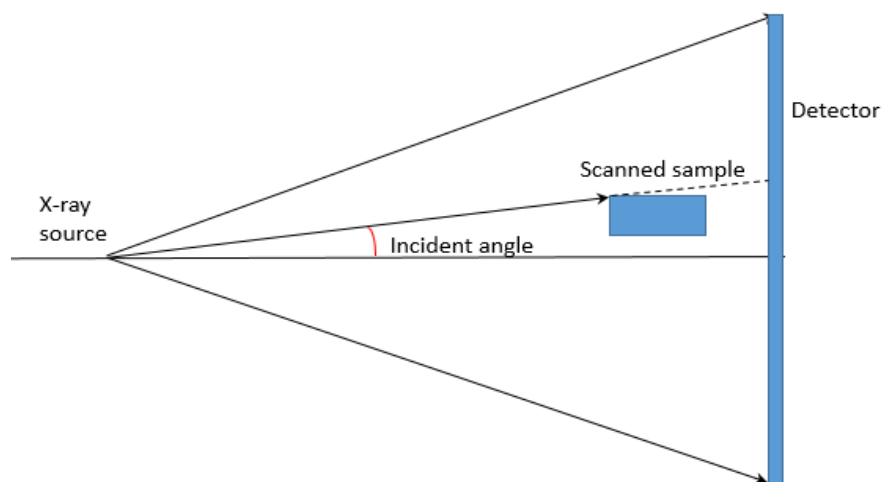


Figure 2.6. Incident angle and the horizontal axis with respect to detector[14]

2.3.3. Geometrical misalignments that leads to errors

Out of all the influencing factors that influence the accuracy of CT measurement system, correcting the geometrical misalignments is of major importance as it describes the complete information of data acquisition and reconstruction on which the further processes has to be carried out. If the errors that occur due to geometrical misalignments are not taken into account, during the reconstruction the further steps that are followed are also affected that leads to artifacts and distortion in the volume that was reconstructed. The figure (2.7) below shows the perfect alignments of the x-ray system using cone beam technique with rotational axis of the turn table where the object is supposed to be placed[15].

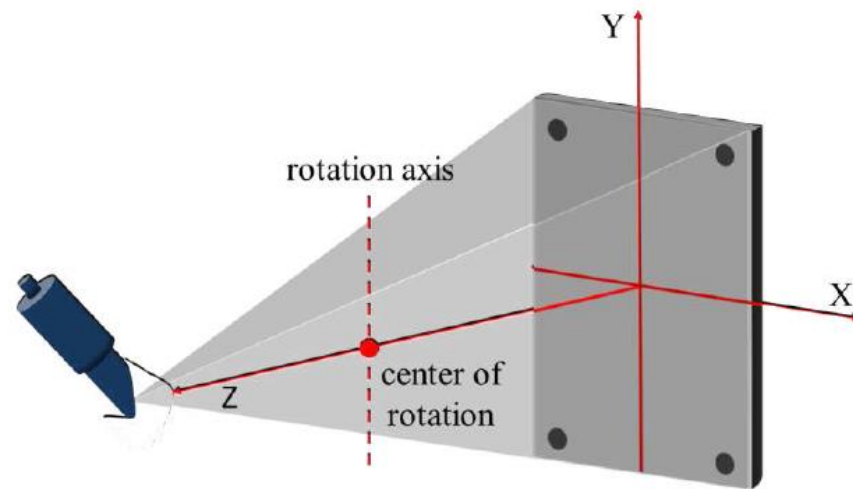


Figure 2.7. Perfectly aligned CT system schematic representation[15]

The geometry of the object contains errors due to the misalignment in the system and imperfection in the mechanical calibration or due to mis-estimation. The mechanical calibration involves the precise calibration of all the axes of the CT system like source to detector and source to rotary table or the object distance. The figure (2.8) shows the misaligned detector position. This calibration is checked routinely for every scan. There are other factors like the positional errors of x-ray source, the object and the detector and also the detectors angular misalignment errors and the centre of rotation errors[15].

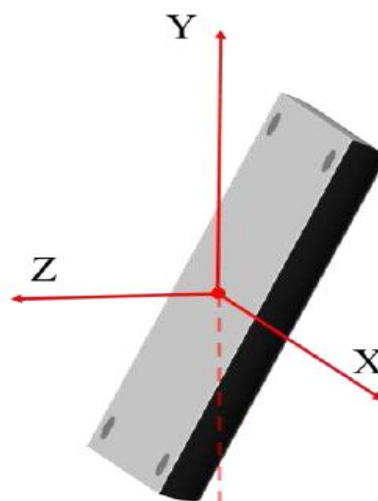


Figure 2.8. Detector angular misalignment[15]

2.4. Need for accuracy assessment

In industries, x-ray computed tomography technique is increasingly being used because of its advantages. The process of reverse engineering has a long path in the history through different approaches like dissection of the system or objects, visual analysis, scanning machines and coordinate measuring machines. But the reverse engineering approach through x-ray computed tomography is still in the path of emerging. As discussed in the above section using CT is more advantageous than using CMM for acquiring the data of the sample. But it is necessary to know how best the results are of reverse engineering using x-ray computed tomography, as the acquired CT data may contain errors or uncertainties. There are many other problems that arise during each step of the workflow like the parameters optimization for x-ray scan, selection of threshold value, noise in CT images, proper selection of surface determination, noise in the meshed file and the converted CAD file may possess errors as well.

During optimization of parameters there should be tradeoff between these x-ray parameters, for example if the voltage is reduced the penetration power reduces, if the voltage or current is increased the resolution decreases optimizing the voltage and current, the time period required for the scan increases. Even the distance at which the object is placed matters the most. After the acquisition of data through XCT, the further steps of reverse engineering are also carefully considered through opting the better parameters which gives better accuracy of the process.

3. Methodology

The flow of this work contains five major steps, as shown in figure (4.1), which are data acquisition, reconstruction, image segmentation, conversion to 3D CAD model and finally the accuracy assessment. The first four steps are under the reverse engineering process while the last step is to assess the accuracy of the process, which is done at each step and at each process.

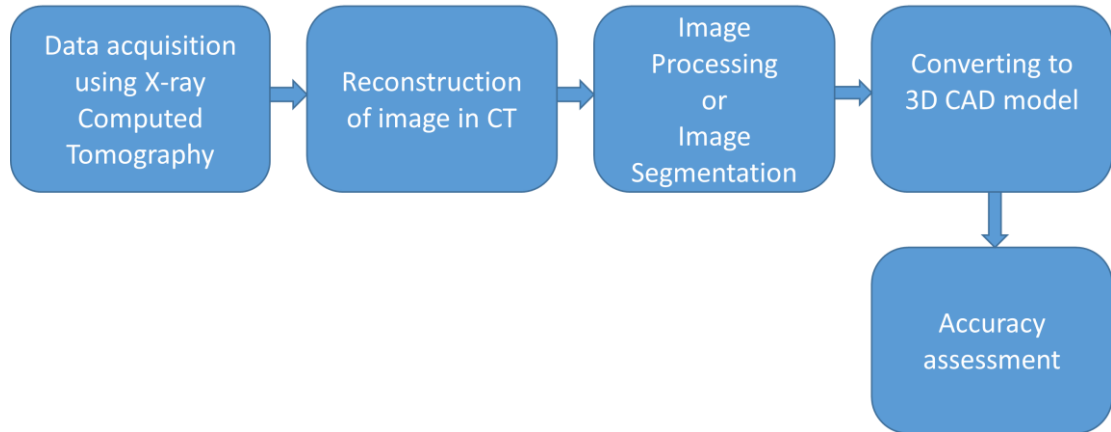


Figure 3.1. The flow graph of the accuracy assessment of a computed tomography based reverse engineering.

The work flow's each step is discussed in the below sections. Each step mentioned contains many small steps to be completed which are also mentioned in these sections.

3.1.Data Acquisition

The data to carry out the process of reverse engineering is acquired by performing computed tomography for the sample. An X-ray computed tomography system consists of an X-ray source, a sample manipulation system, a radiation detector and a computer system to analyze data. X-rays are used to take multiple two dimensional transmission images of an object from different known orientations.

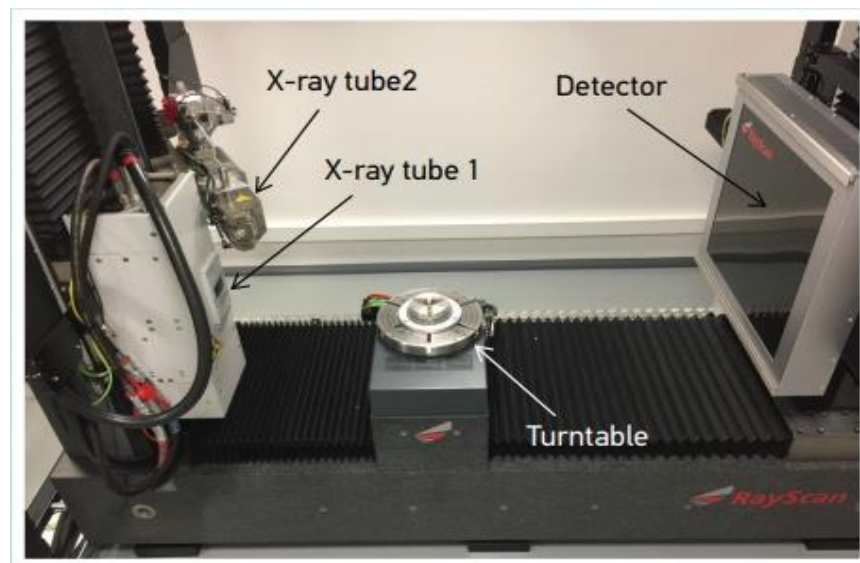


Figure 3.2. Computed tomography experiment setup

Figure (4.2) shows the experimental setup of computed tomography used to acquire the data required for reverse engineering. There are two x-ray sources with a voltage range of 10-230kV and 50-450kV and with the resolution of 3 μ m and 100 μ m respectively. According to the specimen which is to be investigated and the voltage range required, the x-ray source is used. The turntable can rotate 360 degree which helps it to scan the whole sample. The size of the detector is 2048*2048 pixels and the size of the object to be scanned should be less than 600mm/1500mm. There are many parameters that are to be set to obtain the required x-ray images which are given below table. To select the optimized parameters number of scans were performed with different set of x-ray parameters like voltage, current, magnification, position of the object, voxel size and the focus size, to see which may be causing artifacts in the CT data.

3.2. Reconstruction

Reconstruction is a mathematical process to generate the CT images from the obtained scan data. It has the fundamental impacts on the quality of image and the resolution of the image as well. During reconstruction threshold determination is the main parameter which is of concern. The CT images obtained does not only contain the black or white for the background and object respectively, these images contain a scale of grey values from 0 to 65000 with 0 being the value of black and 65536 being the white. The other intermediate grey scale values play an important role in separating the background and object with high precision which helps in surface determination of the object. The software VG Studio MAX uses these voxels of intermediate gray value to find the surface of an object with sub-voxel precision. The reconstruction process in this investigation was carried out automatically as pre-defined by the manufacturer.

3.2.1. Thresholding

Threshold value is a parameter for accurate image segmentation and surface data determination by indentifying edges inside the voxel. Widely used threshold value is ISO-50 (AVG between gray values for air and material). Threshold value can be calculated depending on:

- ✓ The histogram peaks of the scanned material.
- ✓ Based on the region of interest.
- ✓ Based on the distance between the peaks of material and background.

The quality of the CT image can be measured on the basis of grey value histogram and also the measure of degree of separation of the two classes (material and background which is air) in the analyzed CT image. The figure (4.3) below shows the histogram of a CT image which contains one class for the material and the other class for air. The distance that separates the two distributions can be interpreted as the contrast between the classes' distributions. The width of each of the distributions includes the amplitude of the artifacts, noise and the blur of the image. The photon noise is the main cause of the noise present in the CT image and geometric or motion blurring effects that occur during the acquisition of data causes the image blur[16].

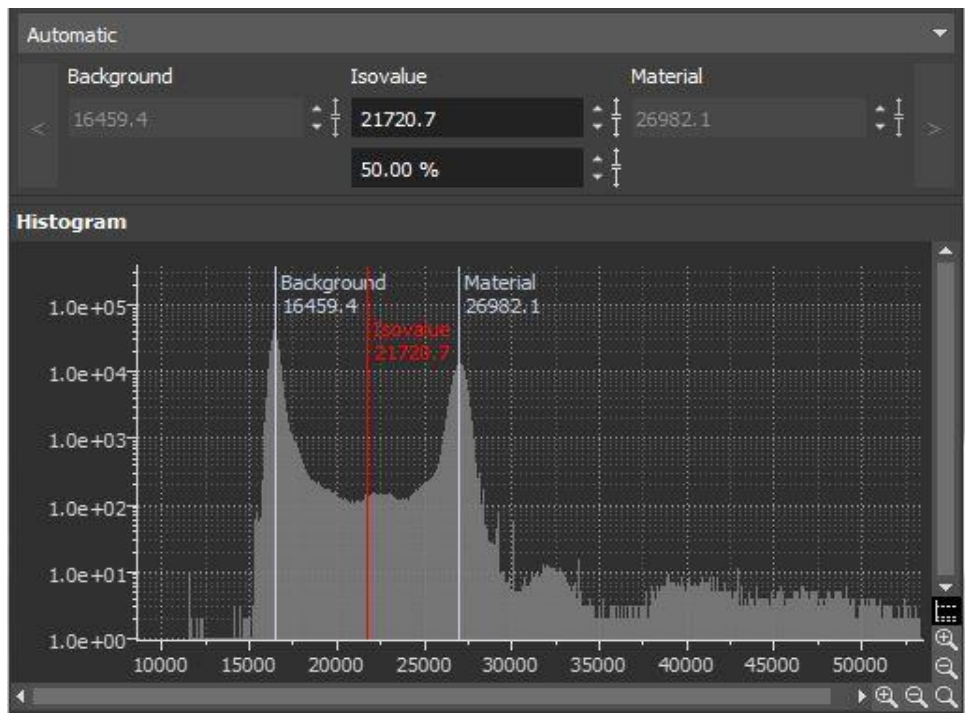


Figure 3.3. Histogram of a CT image

The number of classes can be limited by histogram thresholds and also the borders of the histogram as the number of classes can be greater than two. If the material under investigation is composition of different materials, then different classes can occur in the histogram, two classes are to be selected either automatically or manually by the user. Automatic selection is used in the investigation here which is based on the occurrence probability of the classes. The highest probability of the class in the scanned data will be compared to the class that corresponds to the air. In most cases the normal distributions more than the classes are required to approximate the shape of CT image histograms. Hence, threshold methods which are based on normal distributions are not possible. The alternative solution for this is the histogram minimum “ISO-50%”[16]. The threshold value for the process of image segmentation and surface data determination is calculated automatically by the VGStudio max software.

3.3. Image Processing

This step includes many processes like Surface determination, measuring the samples, analysis and mesh conversion. All these processes are done in the software VGStudio max. First the CT data after scanning process and reconstruction which is done automatically, is imported into the software and the processes mentioned above are carried out which are explained in the below sub-sections.

3.3.1. Surface determination

Surface determination is the process of finding the surface or the outline of the object which acts as the boundary between the object and the background. It is the first process in this step which is done using VGStudio max software. The ISO 50 value was used as default and iterative surface determination is preferred rather than standard surface determination. Standard surface determination gives the material boundary according to the given gray value applied all over the object whereas, iterative surface determination gives a material boundary based on the neighboring

voxels, which greatly compensates for the local deviations that are produced during the scanning process[17].

The isosurface determination done in the VGStudio max software is either based on histogram or on sample background and the material area. The material boundary that is defined by one gray value that is applied globally to the object is the result of the isosurface determination, this surface is called isosurface. In the CT image histogram shown in figure (4.3) the gray value is marked by the red line which is called the isosurface line. This value is the threshold value for the surface determination, the brighter areas are considered as material and the darker areas are considered as the background. The software calculates the boundary of the material by applying trilinear interpolation in subvoxel accuracy[18].

Advanced surface determination was selected with below mentioned parameters:

- Material definition- Automatic which takes ISO 50 between the material and background peaks. The software automatically determines the material and the background peaks in the CT image histogram and then calculates the required gray value for the material boundary.
- Starting contour healing- This option in the surface determination process is used for specific measurements that require the object with surface determined such that small particles outside the object and small voids inside the object are not considered as the surface areas of the object. Remove noise particles option is mostly used during the investigation which removes the noise outside the object.
- Edge threshold – This option allows correcting the starting contour locally by specifying the minimum gray value difference. If the gray value difference is less than this value then the starting contour is used to determine the surface of the object. Automatically calculated value (minimum gray value difference) is used throughout the investigation.

3.3.2. Measuring the samples

After the surface determination process, the samples are measured from the obtained CT data by fitting different shapes according to the requirements like the diameter of the cylinder is measured by fitting a cylinder and calculating its diameter, for example as shown in figure (4.4). This fitting of shapes are done by placing different fitting points according to the required shape and required length.

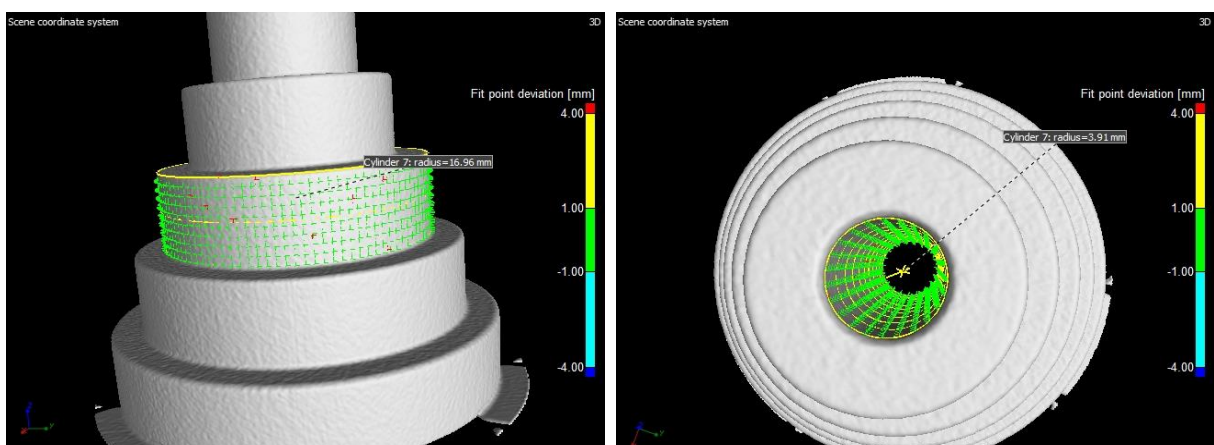


Figure 3.4. Fitting of cylinders to measure the outer and inner diameters

The height of the cylinder is measured by fitting planes and measuring the distance between these planes which is shown in figure (4.5). Likewise any measurements of inner and outer surface of the sample can be carried out by fitting different shapes and measuring different parameters of the fitted shapes or the distance between them.

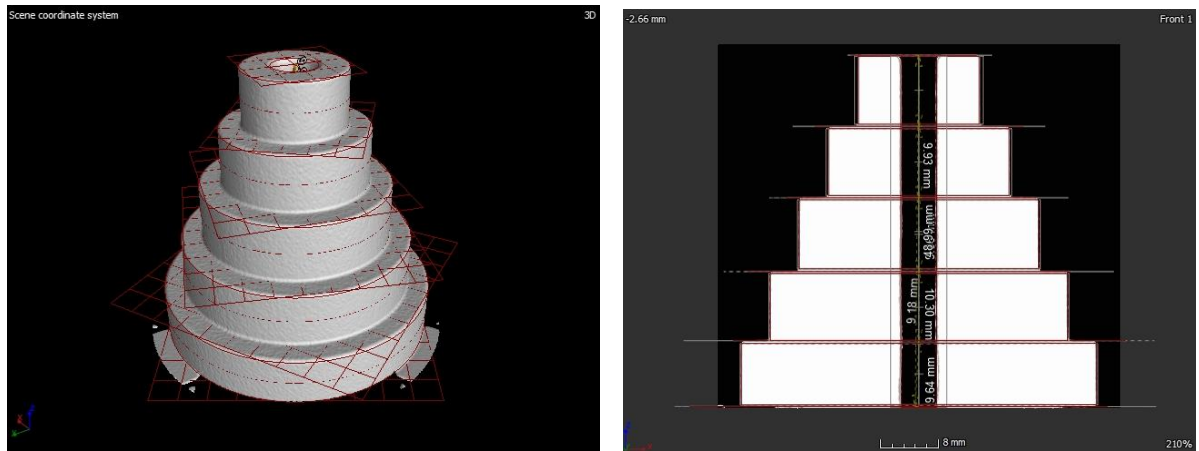


Figure 3.5. Planes fitted in the middle of each step

3.3.3. Gray scale analysis

After measuring the samples to find the measurement accuracy of the process, to find the quality of the CT image gray scale analysis was performed. The gray scale analysis was performed in VGStudio max and MATLAB software. The analysis performed using VGStudio max gave the gray value distribution through color density distribution of the overall object by assigning gray value to different colors. The figure (4.6) below shows the images of gray scale analysis performed in VGStudio max software. The first image shows gray scale analysis performed only for material that is, only the object and the second figure shows the gray scale analysis performed for both background and the object, the respective color scale is shown on the left side of the image.

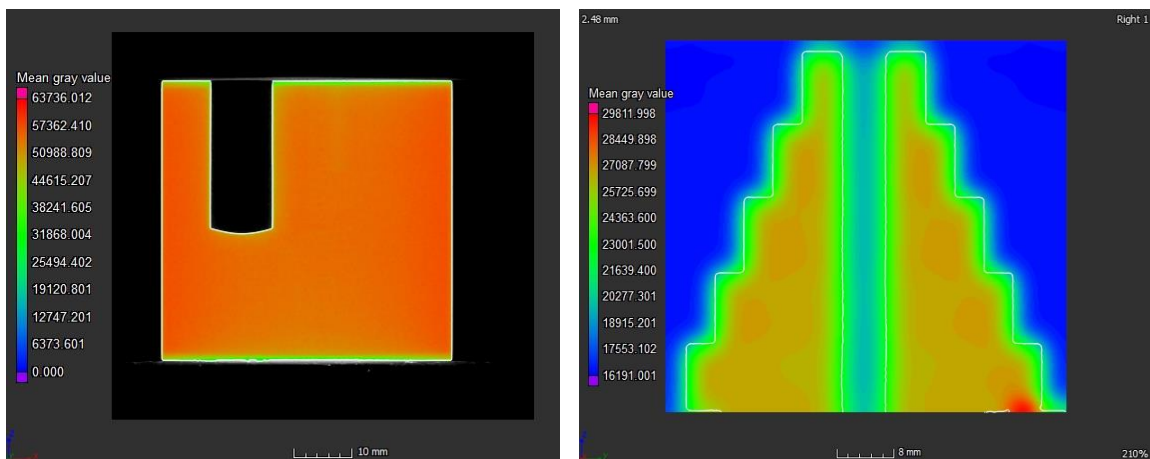


Figure 3.6. Gray scale analysis performed in VGStudio max

Using MATLAB the gray value distribution was obtained for 2D cross sectional image of the object over a pre-defined line[19]. The CT image in 2D was read in MATLAB software and MATLAB functions were used to obtain the gray scale distribution across a desired line which can be drawn

manually or the co-ordinate values could be given indirectly. The figure (4.7) shows the CT image and its respective gray value distribution along the line indicated.

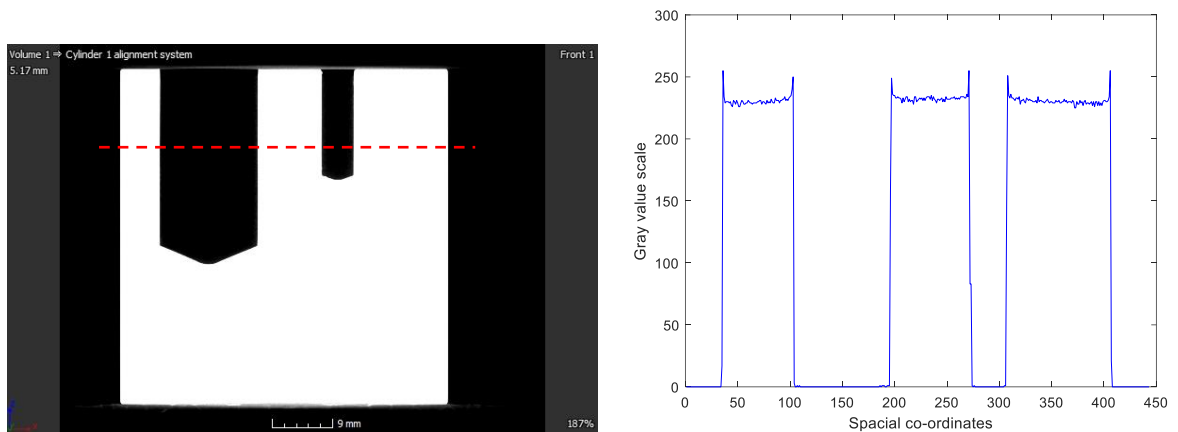


Figure 3.7. gray scale analysis performed in MATLAB

3.3.4. Mesh conversion

After the analysis of the CT data the final process in this step is to convert the CT data into mesh file, as the CT data cannot be converted directly into CAD file. The CT data can be converted into mesh file in the VGStudio max software using the below mentioned parameters:

- Preset selection - This option specifies the preset that is to be applied or to be edited or to be taken as basis for a new preset. Mostly the Ray based fast was selected as the preset as it considers only half volume resolution which makes the conversion faster.
- Surface determination - The determined surface was used where the determined surface of the voxel data set is applied as it defines the surface more precisely than the surface manually defined by the gray value entered.
- Re-sampling mode – This option specifies the sampling distance that is used during the extraction process. The more finer the sampling distance the more data points are generated. Fast re-sampling mode was opted as it gives the result of the conversion process faster than the other options for a trade off with reduced resolution than the resolution of the original data set.
- Point reduction mode – While converting volume data to mesh the point reduction determines which points are on the surface and also makes it possible to exclude points that are not on the surface from the final point cloud. The mode of the point reduction process specifies the tolerance value, the options fast, normal and precise specifies a predefined tolerance value. The figure (4.8) below shows the working of point reduction process.

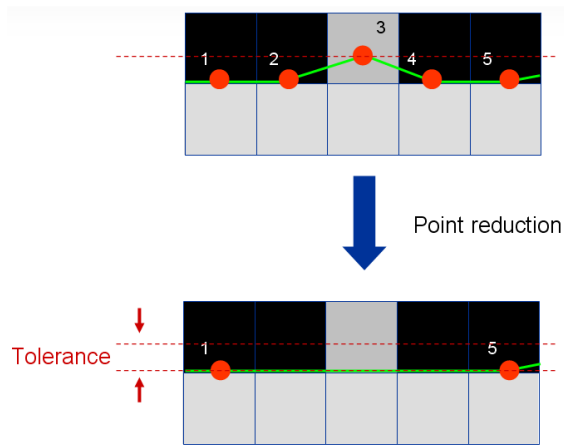


Figure 3.8. Point reduction process[18]

- Simplification mode – The algorithm of mesh simplification combines number of triangles which are aligned in one plane to a larger triangle within the specified tolerance which results in reduced number of triangles, this results in a consequence, the overall dimensions of the final model obtained may slightly vary from that of the original object. But this can be controlled by specifying the simplification mode which gives the tolerance value or the total number of triangles to be obtained. The options high simplification and high precision which were used in this investigation provides predefined settings. The figure (4.9) below shows the triangles formed during conversion process with and without simplification[18].

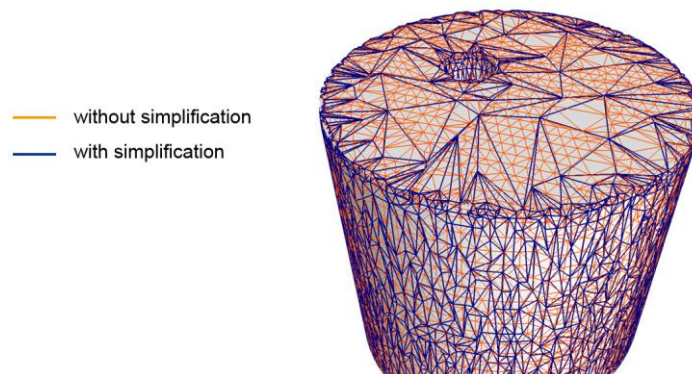


Figure 3.9. Mesh simplification[18]

3.4. Conversion to 3D CAD model

After surface determination, measuring the samples and gray-scale analysis the CT data of samples are then meshed to carry out the next step that is conversion to 3D CAD model. The meshed samples were exported as STL files which are then imported in the software SolidWorks to convert them into 3D CAD models; with this step the process of reverse engineering is complete. The CAD files obtained are also measured to find out the accuracy of the whole process.

3.5. Accuracy assessment

The accuracy of the whole reverse engineering process using XCT approach is assessed. Accuracy assessment is done at different stages of the process, the measurement accuracy is done after the measurements of the CT data are carried out by calculating the deviation in terms of percentage, of

the measurements with respect to the original sample measurements used at the stage of sample designing. The below equation (5.1) was used to find out the percentage deviation.

$$\text{Percentage deviation or accuracy} = \frac{V_0 - V_A}{V_A} \times 100\% \quad \text{----- (4.1)}$$

Where, V_0 is the measured CT value and V_A is the acceptable value, here the measurement carried out using CMM. The samples are measured using co-ordinate measuring machine, deviations are calculated with respect to the CT measurements. The different CT measurements deviations are also compared with each other to obtain the best parameter set. Finally after the CAD files are obtained these CAD measurements of the sample are also compared with the CT measurements. Not only measurement accuracy is assessed, but also the accuracy of the CT data obtained. For XCT approach the quality of the gray image or the CT image obtained is most important, hence the gray scale analysis is done for different CT data obtained for different parameter sets to choose the best parameter set which gives the accurate result for reverse engineering process.

4. Experimental investigations

4.1. Samples used for the experiment

The experiment was carried out for four samples which are shown in below figures, according to the steps explained in the above section. Special samples from Plexiglas were produced according to the CAD drawings and scanned using x-ray computed tomography system. The first sample is a plane cylinder made out of plexiglass with 50mm diameter and 50mm height as shown in figure (5.1). This sample was rather considered a simple one on purpose as to see how the process can be carried out.

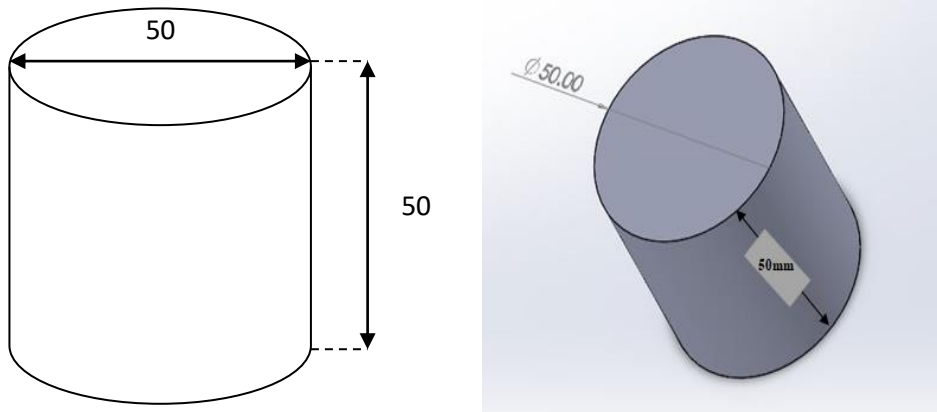


Figure 4.1. Sample1-Plexiglass cylinder with dimensions

The second sample is similar to the first one except that it has three holes of different diameters and heights, that are 5mm, 10mm and 15mm and different heights 15mm, 35mm and 25mm inserted in it which are as shown in below figure (5.2). This sample was made a little complex to see the progress of the process.

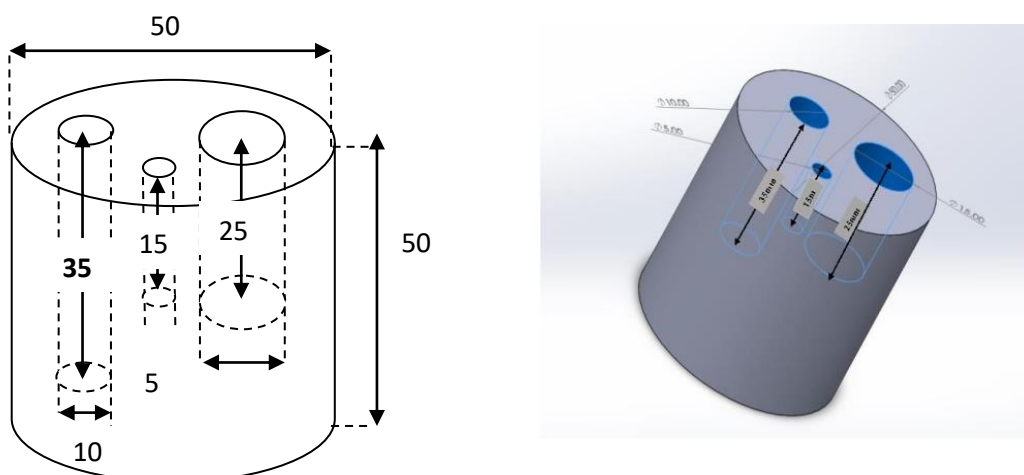


Figure 4.2. Sample2-Plexiglass cylinder with holes and its measurements

To understand the influence of shapes and the material used to produce the sample, the other two samples, sample3 and sample4 was considered for experiment. Both sample3 and sample4 are the step cylinders consisting of 5 steps with the dimensions (in mm) as shown in below figure (5.3), but

sample3 is made of plexiglass and sample4 is made of aluminum[20]. The sample was first designed as a CAD file in Solidworks software and the same was produced.

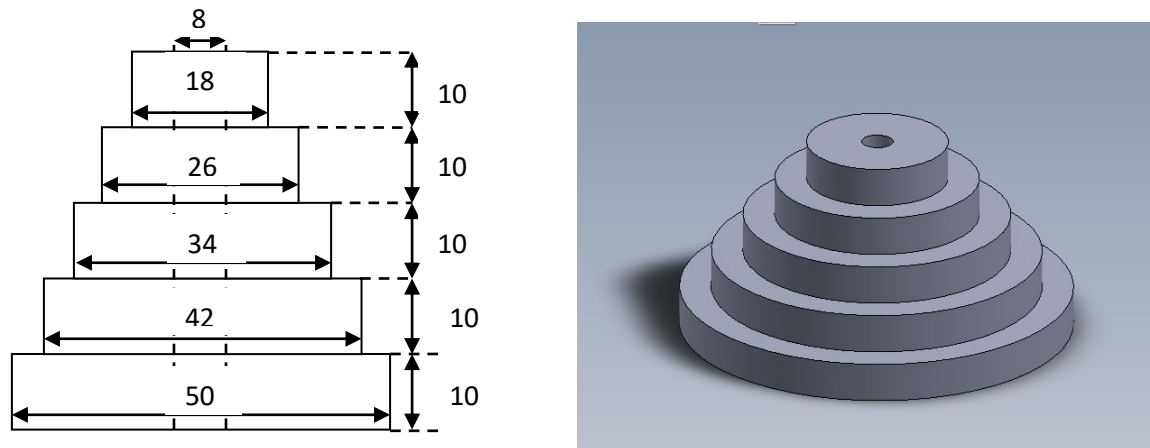


Figure 4.3. Step cylinder with dimensions

4.2. X-ray parameters

For the first step, data acquisition through XCT, the parameters for the scan had to be set. The table (5.1) shows the two CT scan parameters. These parameters were used to scan the sample1 and sample2.

Table 4.1. XCT scanning parameters used for sample1 and sample2

Parameters	Scan 1	Scan 2
Voltage	110 kV	
Current	200 uA	
Power	22 watts	
Focus size	31 um	
Integration time and Averaging	3000 and 3 ms	
Number of Projections	2970	
Voxel size	100 um	32.19 um
Distance from source to object	758.262 mm	244.11 mm

The experiment was carried out to find out the influence of shape on the process of reverse engineering. The plexiglass step cylinder sample (figure 5.3) was scanned many times using x-ray computed tomography with different parameters. A total of twelve CT data files were obtained with twelve different parameter sets of x-ray scanning. Each CT data was carried out the process of reverse engineering. The below table (5.2) presents the x-ray parameter sets used for scanning to obtain the CT data[21].

Table 4.2. XCT scanning parameters used for plexiglass step cylinder (sample3)

X-ray parameters	Magnification	Voltage	Current	Average time	Voxel size	Focus size
Scan1	Mg1_25	100 kV	200 uA	666 ms	160 um	10 um
Scan2	Mg2	100 kV	200 uA	666 ms	100 um	10 um
Scan3		200 kV	200 uA	666 ms	100 um	42 um
Scan4	Mg2_5	100 kV	100 uA	2000 ms	80 um	6 um
Scan5		100 kV	200 uA	2000 ms	80 um	10 um
Scan6		100 kV	200 uA	600 ms	80 um	10 um
Scan7		200 kV	200 uA	600 ms	80 um	42 um
Scan8	Mg5	100 kV	200 uA	666 ms	40 um	10 um
Scan9		100 kV	200 uA	600 ms	40 um	10 um
Scan10		100 kV	200 uA	2000 ms	40 um	10 um
Scan11		200 kV	200 uA	666 ms	40 um	42 um
Scan12		200 kV	200 uA	600 ms	40 um	42 um

The investigation for aluminum step cylinder (figure 5.3) was carried out to find out the accuracy of the process for different materials, as previously the analysis was carried out for the plexiglass material. The CT scan data were obtained for the aluminum sample for different set of x-ray parameters to check the accuracy. The table (5.3) below shows the different x-ray parameter sets used to obtain the CT data.

Table 4.3. XCT scanning parameters used for aluminum step cylinder (sample3)

X-ray parameters	Magnification	Voltage	Current	Average time	Voxel size	Focus size
Scan1	Mg2_5	200 kV	200 uA	1000 ms	80 um	10 um
Scan2		200 kV	200 uA	600 ms	80 um	10 um
Scan3		100 kV	200 uA	2000 ms	80 um	10 um
Scan4	Mg5	200 kV	200 uA	1000 ms	40 um	42 um
Scan5		200 kV	200 uA	600 ms	40 um	42 um
Scan6		100 kV	200 uA	2000 ms	40 um	10 um

4.3. Surface determination

After the process of data acquisition, the next step was reconstruction which is done automatically by the software of the XCT system. The next process was surface determination which was done

according to the parameters mentioned in the above section. The figure (5.4) below shows surface determined sample of CT image. The white line in the figure represents the boundary between the sample and the background[22].

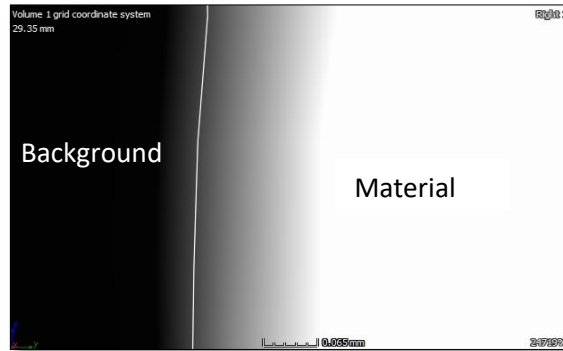


Figure 4.4. The surface determined CT image

4.4. Gray scale analysis

4.4.1. Gray scale analysis of Sample2

As the experiment is carried out in CT system, the gray value distribution in the CT images gives a lot of information about the quality of the CT data obtained. The gray scale analysis was first performed in the VGStudio max software, which gave the results in terms of color distribution representing particular gray value with a particular color. Sample2 was considered for the analysis, where both the CT data obtained using the scan1 and scan2 parameter sets were analyzed which is shown in the figure (5.5 and 5.6) below. The whole cylinder was not considered for the analysis as the analysis of whole cylinder of scan1 data took a huge amount of time; hence a 5mm length from the top surface of the cylinder was considered for both the data. The color scale in the picture shows the color code for the average gray value distribution. It is evident that the distribution in the CT image of scan1 at the surface has low average gray value compared to the surface gray value distribution of CT image of scan2. Both the figures 3D and 2D views show the presence of noise at the top surface of the sample2 scan1 data.

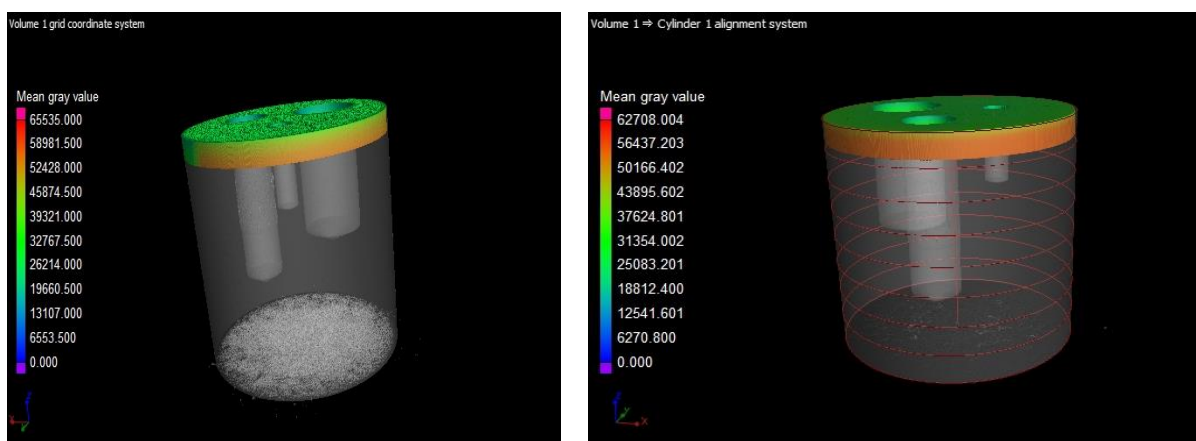


Figure 4.5. 3D view of gray value density distribution of a part of 5 mm from the top surface where (a) sample2 scanned using scan1 parameters and (b) sample2 scanned using parameters of scan2

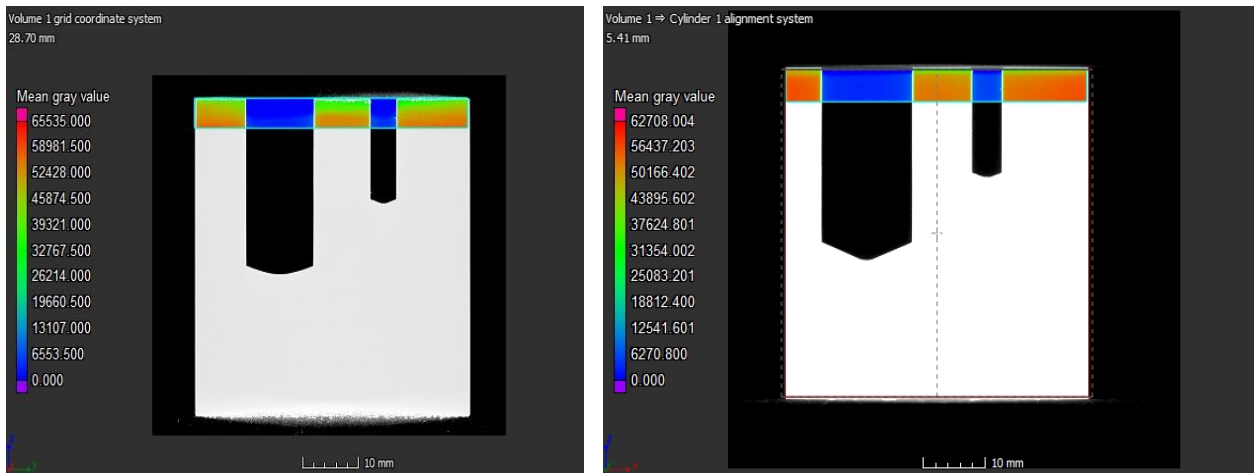


Figure 4.6. 2D view of gray value density distribution of a part of 5 mm from the top surface where (a) sample2 scanned using scan1 parameters and (b) sample2 scanned using parameters of scan2

The above analyses are obtained considering the average of the surface area at which the analysis is performed. For better understanding the images were imported to MATLAB software and then performed image processing to find the gray value distribution over a pre-defined line, which is shown in the below figure (5.7) for both CT images of scan1 and scan2 respectively. The distribution is quite stable in the case of CT image of scan2 than CT image scan1 which has the disturbing distribution graph across the edges.

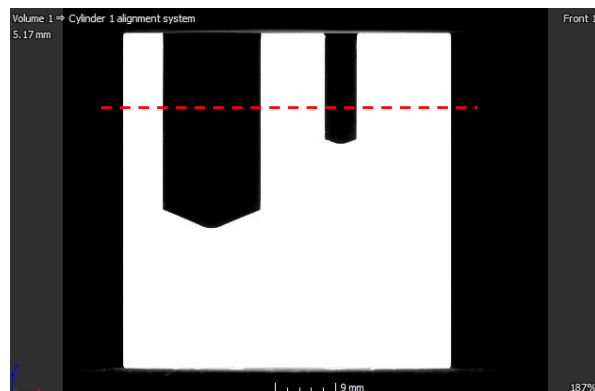


Figure 4.7. The gray scale image showing the line across which the gray value distribution is plotted

According to the defined line shown in figure (5.7) the plot of gray value distribution is shown in figure (5.8) for scan1 and scan2 CT images. The distribution graph of CT image of scan2 has a flat top which represents the surfaces across the line, this concludes that this CT image has proper surface determination and is free from most of the artifacts. Whereas the gray value distribution of the first image, that is CT image of scan1 has disturbances at the surfaces.

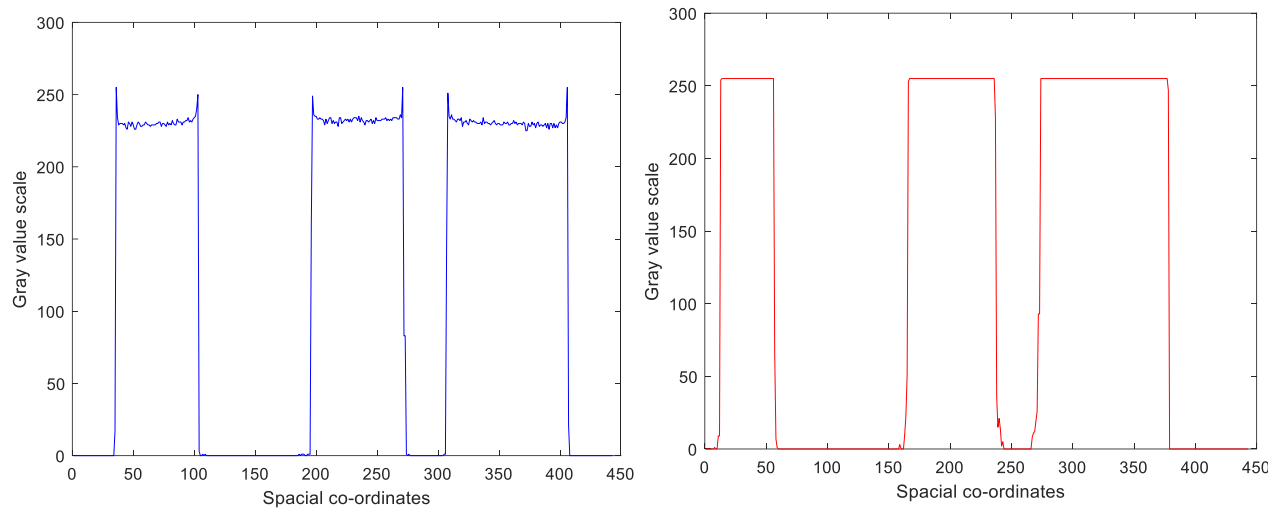


Figure 4.8. The gray value distribution plot of pre-defined line of scan1 and scan2 respectively

4.4.2. Gray scale analysis of sample3

For the sample3 (plexiglass step cylinder), the CT images were processed using MATLAB software, where gray value distribution curves were obtained. From these graph the surface determined can also be judged, the gray value distribution can also tell the quality of the data acquisition process also. The gray value distribution curves were obtained for each of the CT images of different scans along the pre-defined line. These curves give better understanding in comparison of each of the CT data of the step cylinder. The figure (5.9) below shows the CT image which has the pre-defined line along which the gray value distribution curve is obtained. The gray value distribution curves are plotted according to table (5.2) of parameter sets.

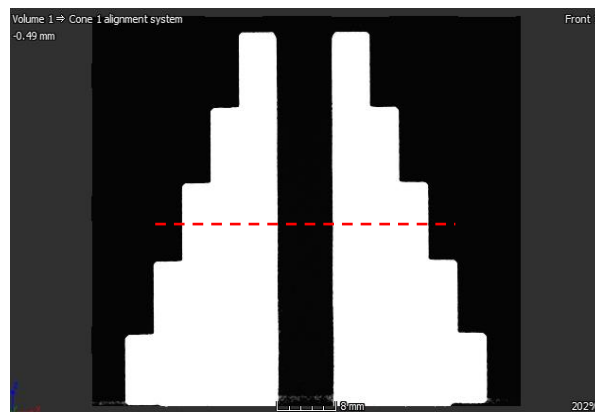


Figure 4.9. CT image showing the predefined line

The first parameter set is of magnification1.25, the gray value distribution curve was plotted along the line as shown in figure (5.9), which passes through centre of the third step of the cylinder. The gray value distribution curve is shown in the figure (5.10) below, which has the exact flat surface edges indicating the perfect CT image with proper surface determination. This can be due to the high voxel size and low magnification values used for the scan.

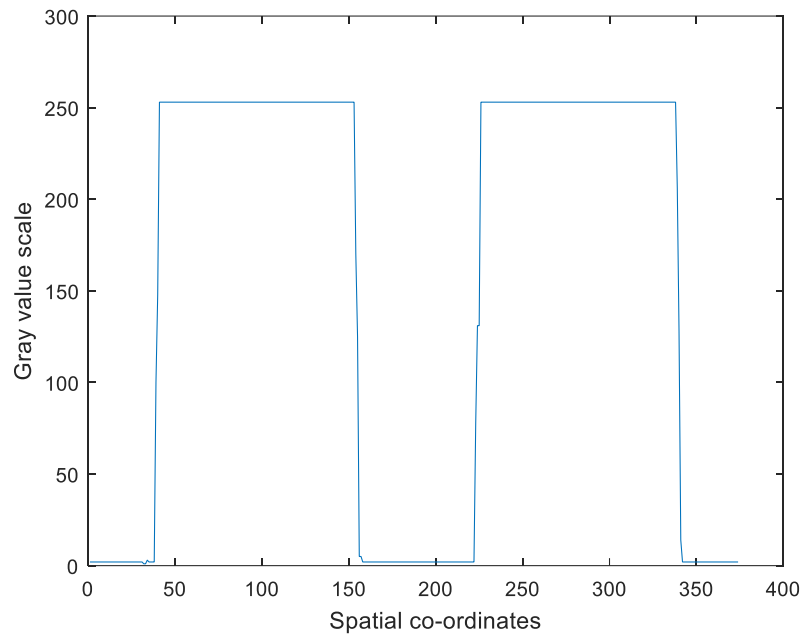


Figure 4.10. Gray scale distribution for the first parameter set with magnification_1.25

The next gray value distribution curves are shown in figure (5.11) below, with magnification₂. The gray value distribution curve was plotted along the line as shown in figure (5.9), which passes through centre of the third step of the cylinder. The curve of scan2 parameter set has the exact flat surface edges indicating the good quality of CT image with proper surface determination. This can be due to the high voxel size and low magnification values used for the scan. The scan3 parameter set gray value distribution plot has disturbance which indicates the improper gray value distribution along the step cylinder. The CT image here has low resolution due to high voltage input used for the scan.

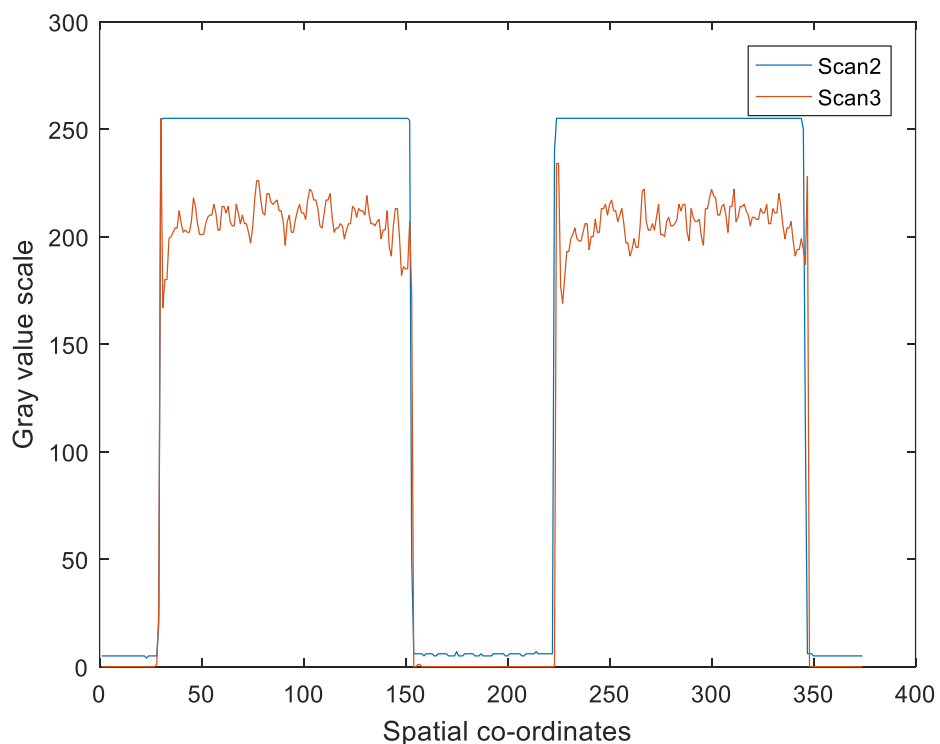


Figure 4.11. Gray scale distribution for the parameter sets with magnification₂

The next gray value distribution curves are shown in figure (5.12 and 5.13) below, with magnification2.5 and magnification5. According to the 2D line shown in figure (5.9) all the gray value distribution curves were plotted. The curves of scan4, scan5, scan6 and scan7 parameter sets having the same magnification value of 2.5 are shown in figure (5.12), all the curves have the exact flat surface edges indicating the good quality of CT image with proper surface determination. In these sets scan7 has high voltage but less voxel value trades-off with it.

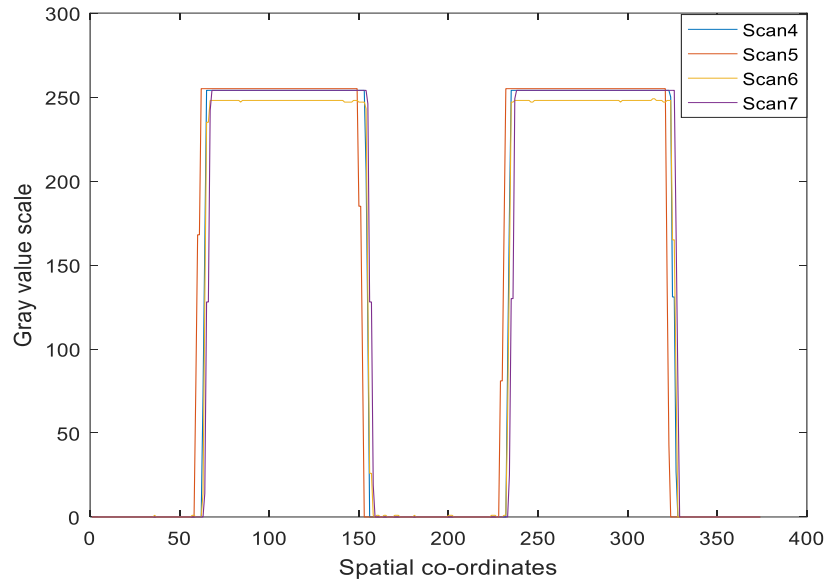


Figure 4.12. Gray scale distribution for the parameter sets with magnification_2.5

The curves of scan8, scan9, scan10, scan11 and scan12 parameter sets having the same magnification value of 5 are shown in figure (5.13), all the curves have the exact flat surface edges except for the orientation of the graphs as each CT image has different number of pixels. The flat surface indicates the good quality of CT image with proper surface determination, as the parameter set does not have much difference in the main parameters like the voltage, voxel size and the magnification.

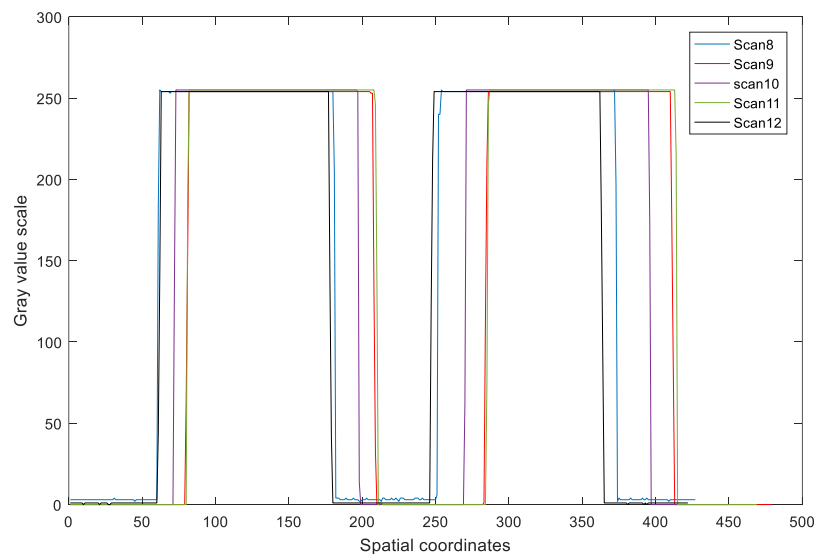


Figure 4.13. Gray scale distribution for the parameter sets with magnification_5

4.4.3. Gray scale analysis of sample4

For the aluminum step cylinder, sample4 (plexiglass step cylinder), the CT images were processed using MATLAB software, where gray value distribution curves were obtained. These curves give the result of not only how well the surface determination was carried out but also the quality of the data acquired. The gray value distribution curves were obtained for each of the CT images of different scans along the pre-defined line shown in figure (5.14). These curves give better understanding in comparison of each of the CT data of the step cylinder. The gray value distribution curves are plotted according to table (5.3) of parameter sets.

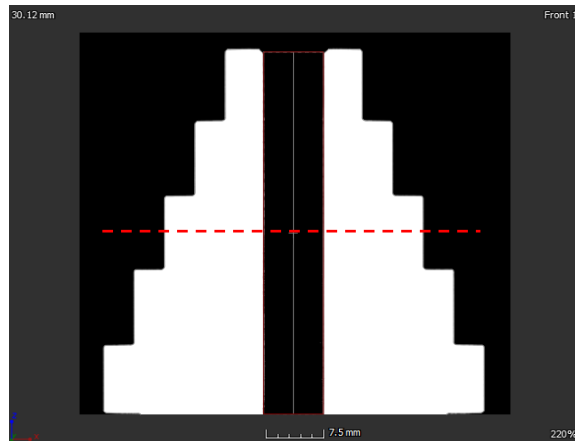


Figure 4.14. CT image of aluminum step cylinder showing the pre-defined line

The figure (5.15) below shows the gray value distribution curves of the parameter set with magnification 2.5, which are scan1, scan2 and scan3. All the curves have a flat surface except for the orientation of the graphs as each CT image has different number of pixels, concluding that the CT data acquired are of good quality and also with a better determined surface.

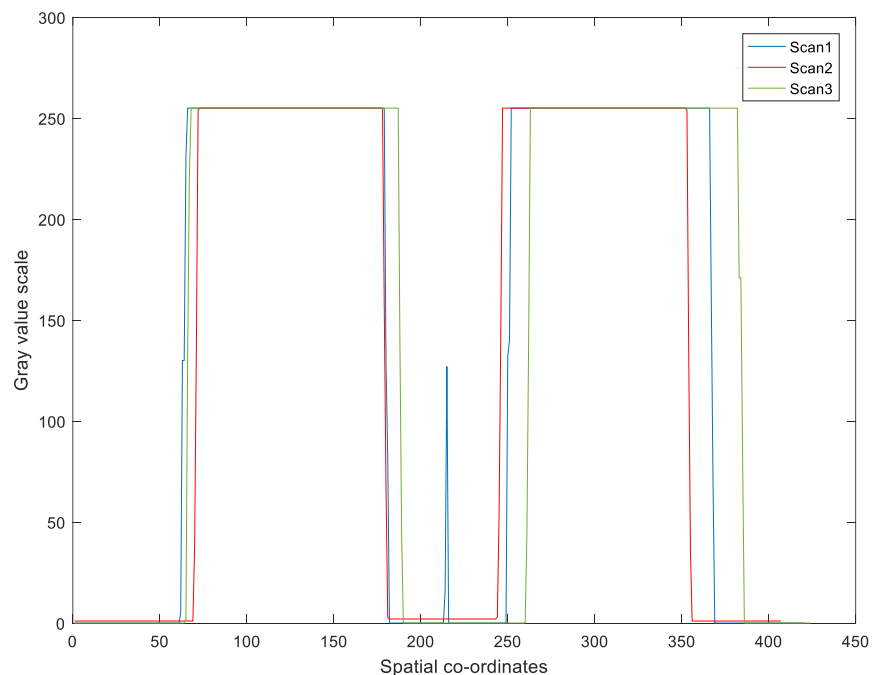


Figure 4.15. Gray scale distribution for the parameter sets with magnification_2.5

The figure (5.16) below shows the gray value distribution curves of the parameter set with magnification 5, which are scan4, scan5 and scan6. All the curves have a flat surface except for the orientation of the graphs as each CT image has different number of pixels, concluding that the CT data acquired are of good quality and also with a better determined surface.

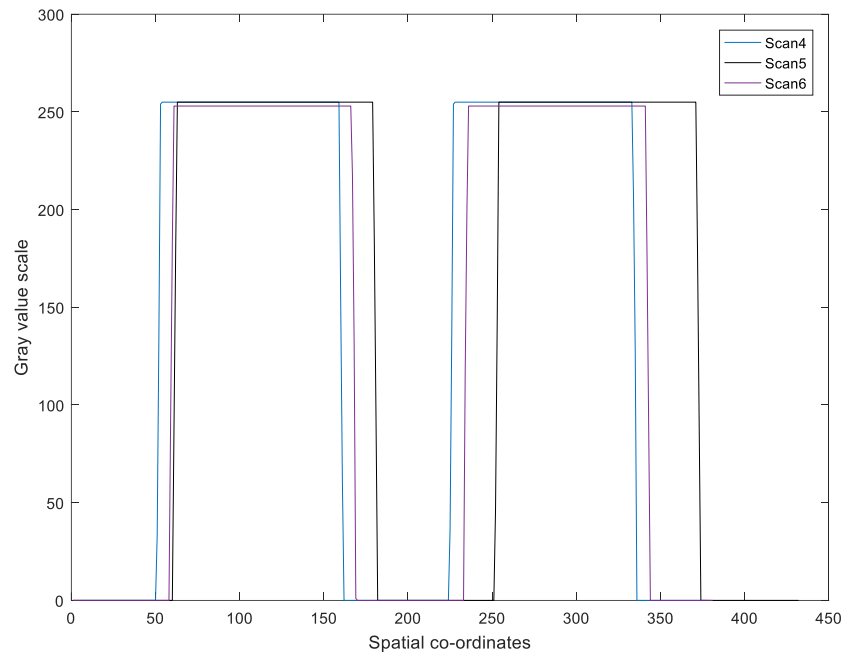


Figure 4.16. Gray scale distribution for the parameter sets with magnification_5

Although the gray value distribution curves were obtained for all the parameter sets, they were obtained only over a single line that is in the middle of the cylinder, through the third step. To confirm that the gray value distribution of the whole cylinder in the CT image was the same, the curves were plotted at each step of the cylinder. For this purpose the CT image with noise present in it was considered which is shown in the figure (5.17) below along with the pre-defined lines at each step across which the curves were plotted.

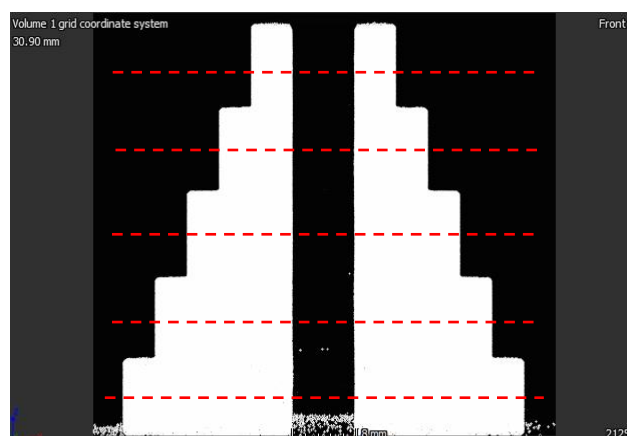


Figure 4.17. CT image of step cylinder showing the pre-defined lines

The curves plotted are shown in the figure (5.18) below, all the curves show flat top surfaces at each step. This shows that the quality of the CT image is acceptable and is the better approach for the process of reverse engineering.

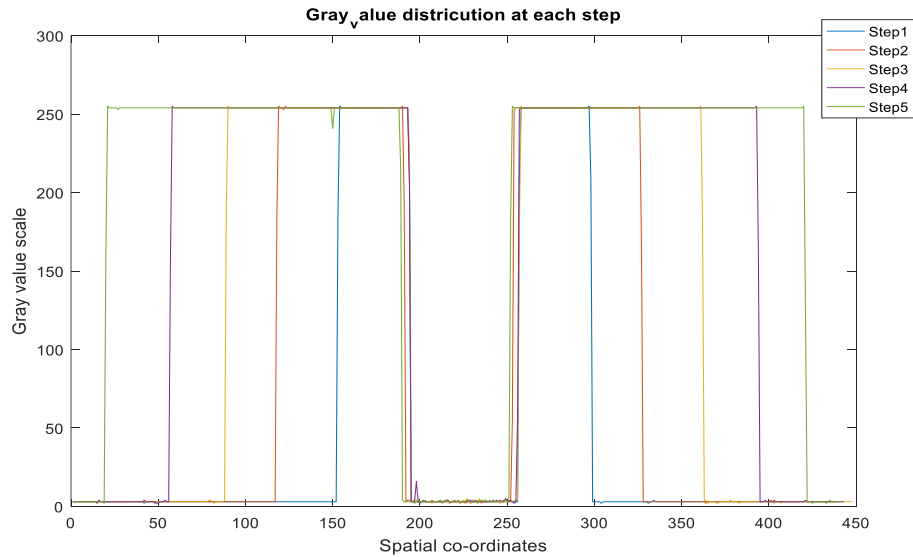


Figure 4.18. Gray scale distribution at each step of the step cylinder

4.5. Measurement of the sample

After surface determination the samples were measured using the CT images by fitting different shapes.

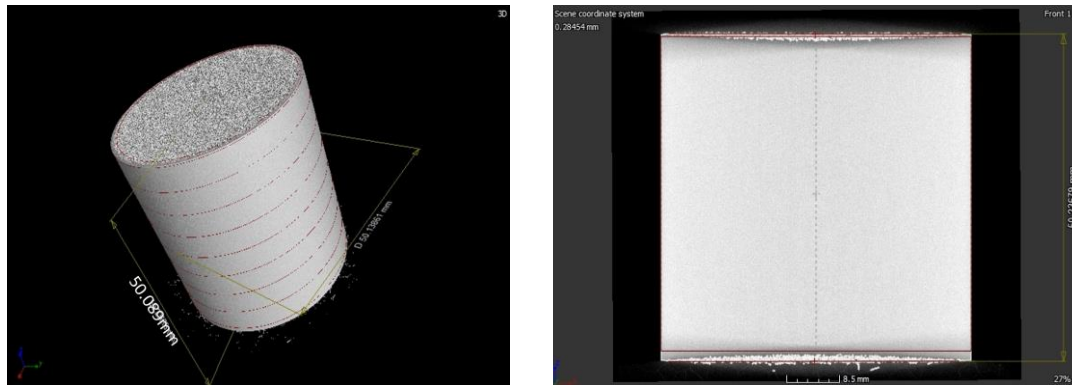


Figure 4.19. CT images of sample1. (a) 3D view (c) Front view

The CT images shown in figure (5.5 and 5.6) are of the sample1 and sample2 respectively, which are obtained after the process of surface determination and measuring the samples in the CT scan. These images contain artifacts which act as noise that reduces the overall accuracy of reverse engineering.

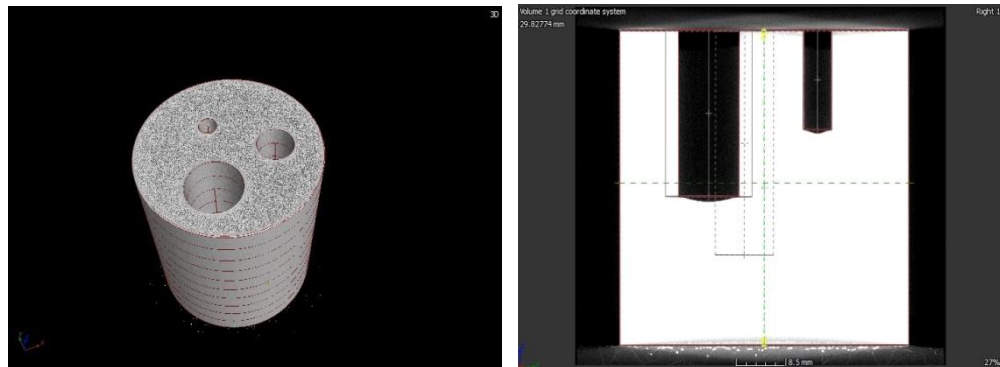


Figure 4.20. CT images of sample2 with noise (a) 3D view (b) Right view

These artifacts are caused by cone beam error that is the object is not placed at right position for an optimized incident angle between the x-ray beam and the object. This noise affects the further processes as well. To overcome these noise many options of surface determination were applied. The table (5.4) shows the measurements of the same CT data performed with different surface determination parameters.

Table 4.4. Iterations of surface determination with automatic and advanced settings

Starting contour healing	Diameter	Height
Remove noise particles	50.14 mm	49.97 mm
Remove small voids	50.13 mm	50.09 mm
Remove all voids	50.14 mm	50.016 mm
Remove noise particles and small voids	50.14 mm	50.24 mm

The below figure (5.7) shows the CT images of the sample2 with the parameters mentioned as scan2 in table (5.1). These parameters differ in the distance at which the object is placed from the detector. This optimization has reduced the artifacts in the CT images. This reduced the time for further processes of surface determination and mesh conversion to a large extent, where the process of surface determination used to take from 20 minutes to 2 hours had reduced to 8 to 10 minutes and the process of mesh conversion used to take from 6 hours to 2 days had drastically reduced to less than a minute.

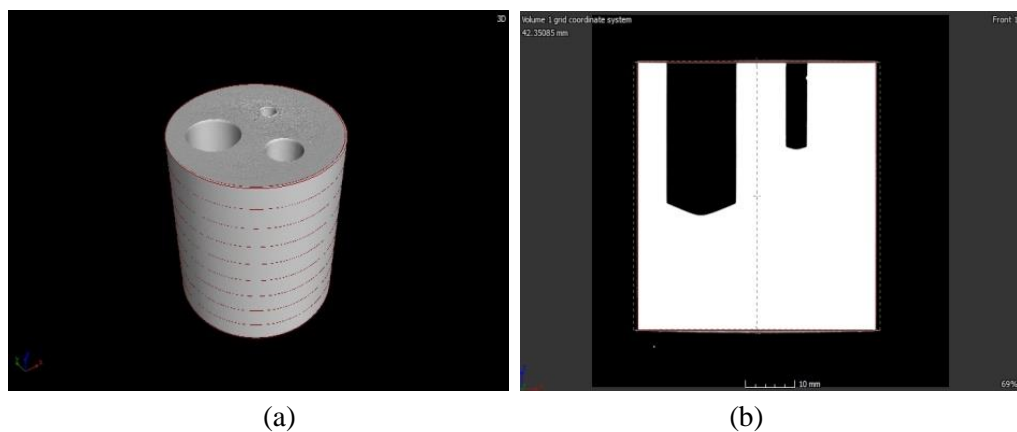


Figure 4.21. CT images of sample2 with reduced noise (a) 3D view (b) Right view

The CT image of the sample3 (plexiglass step cylinder) is shown in figure (5.8 and 5.9). The CT image in figure (5.8) is basically free from noise from visual perspective which was scanned using scan2 parameter set of table (5.2).

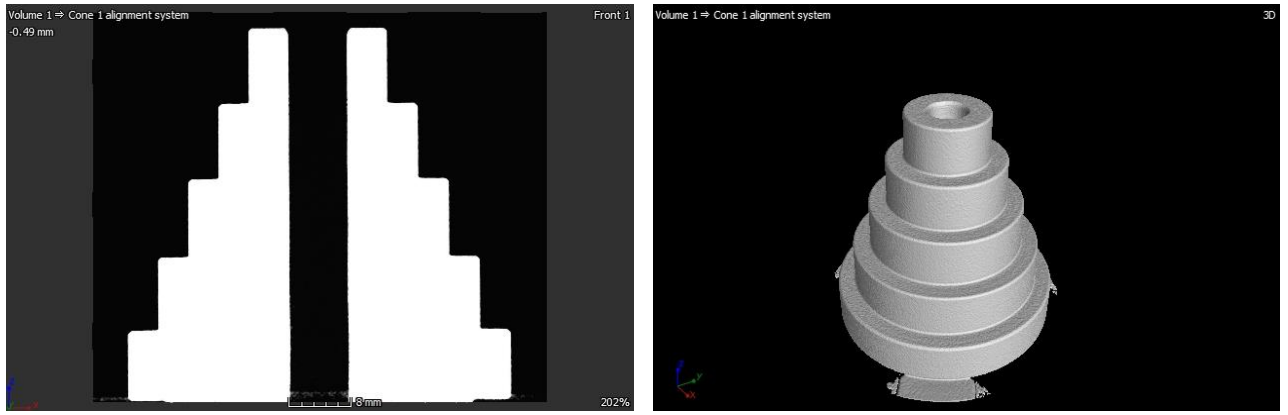


Figure 4.22. CT images of sample3 without noise (a) Right view (b) 3D view

The reconstructed CT images obtained after scanning from scan8 parameter set of table (5.2) contains noise which is visible in figure (5.9) below. This can be due to the low voxel size of 40 μm and even the high magnification (5). But the image resolution is good as the voltage used is 100 kV.

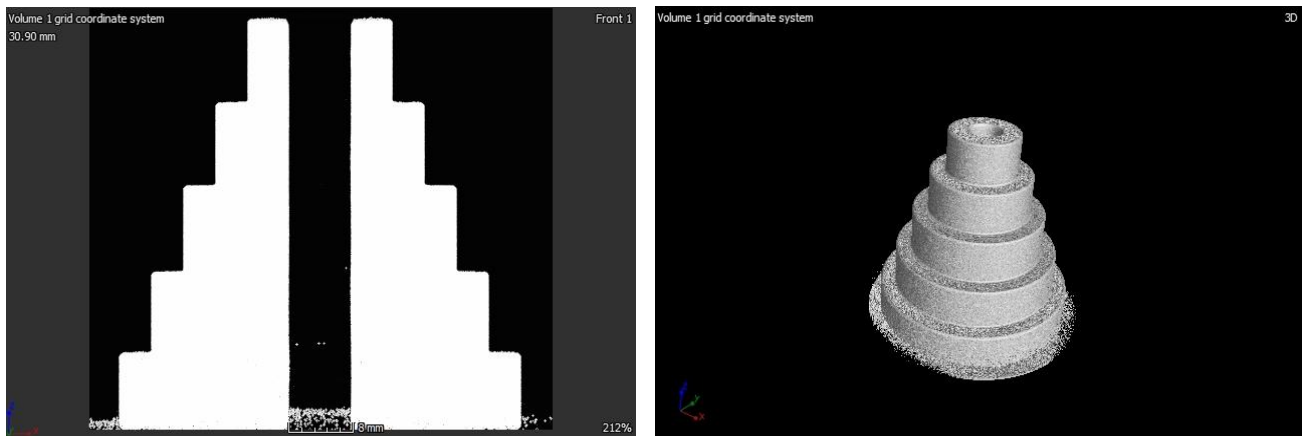


Figure 4.23. CT images of sample3 with noise (a) Right view (b) 3D view

The sample4, aluminium step cylinder was also scanned by the parameter sets shown in table (5.3). The CT images, after the process of surface determination and measuring the samples, are shown in figure (5.10). The artifacts are absent as discussed above. This helped in accurate determination of the surface and gave almost accurate measurements of the sample as well.

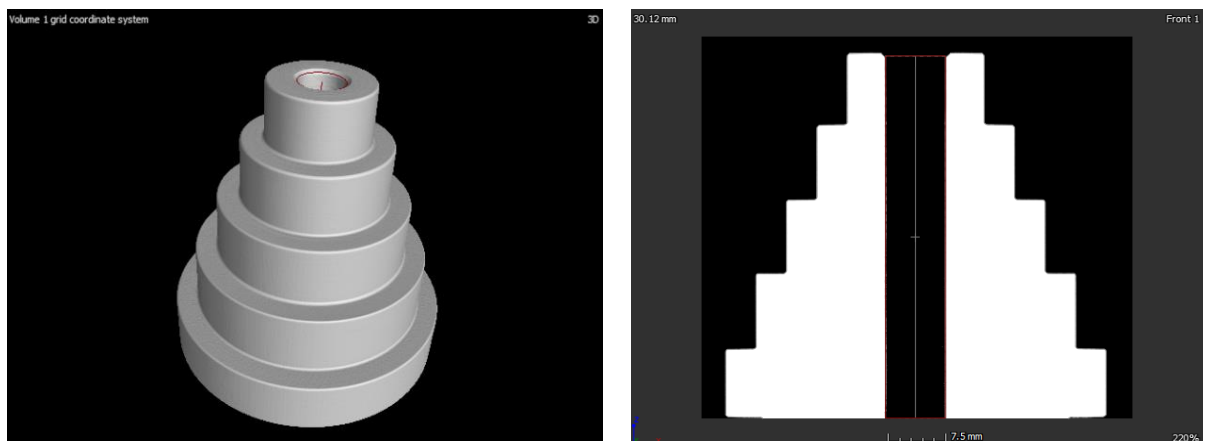


Figure 4.24. CT images of sample4 (a) Right view (b) 3D view

4.5.1. Measurement results

The measurements of the sample were tabulated to find the percentage deviation from that of the original sample measurements. The original samples were measured using mitutoyo measuring machine (CMM).

The sample1 had no much measurements to be done hence it is neglected. The sample2 measurements are shown in table (5.5). The table gives the measurements of the original CAD design, the sample produced, the measurements of CT images and the percentage deviation. The two parameter sets are considered for the measurements for comparison.

Table 4.5. Measurement results of Sample2

Measurements of:	CMM measurements	CT data using scan1	% deviation	CT data using scan2	% deviation	Converted CAD design of scan2	% deviation
Diameters of the holes	4.99	5	0.20%	4.99	0.00%	5.17	3.61%
	10.04	10.05	0.10%	10.09	0.50%	10.31	2.69%
	14.98	15	0.13%	15	0.13%	15.22	1.60%
Cylinder diameter	50.18	50.13	-0.10%	50.67	0.98%	50.1	-0.16%
Height of the holes	-	15.06	0.40%	15.55	3.67%	15.17	1.13%
		26.43	5.72%	26.32	5.28%	26.24	4.96%
		35.69	1.97%	35.45	1.29%	35.68	1.94%
Cylinder height	50.06	50.06	0.00%	49.98	-0.16%	50.01	-0.10%

For better understanding the tabulated values were plotted with the measurements in mm against the deviation values in percentage. The figure (5.25) below shows two graphs, on which shows the diameters v/s its deviation and the other heights v/s its deviations. The first figure has three plots, CT scan1 measurements, CT scan2 measurements and the final CAD converted sample measurements, from these plots the CT scan1 measurements has a very low deviation compared to all other but the CT data obtained using scan1 could not be interpreted further as the later processes were not been completed because of the noise present in the CT data, scan2 measurements are also acceptable as the deviation is very low. The second figure has three plots which are CT scan1 measurements, CT scan2 measurements and the final CAD converted sample measurements. Comparing the curves the scan2 data plot has least error or deviation in the measurements. Hence in this case the scan2 x-ray parameter set with 110kV voltage, 200uA current, 22 watts power, focus size of 31 um, voxel size of 32.19 um and with a distance of 244.11mm from source to object is considered the optimal parameter set. Here the CMM measurements are absent as it was not possible to measure the heights of the holes in the cylinder without dissecting it, hence the original sample measurements were used instead for deviation calculation. This highlights the advantage of CT approach here.

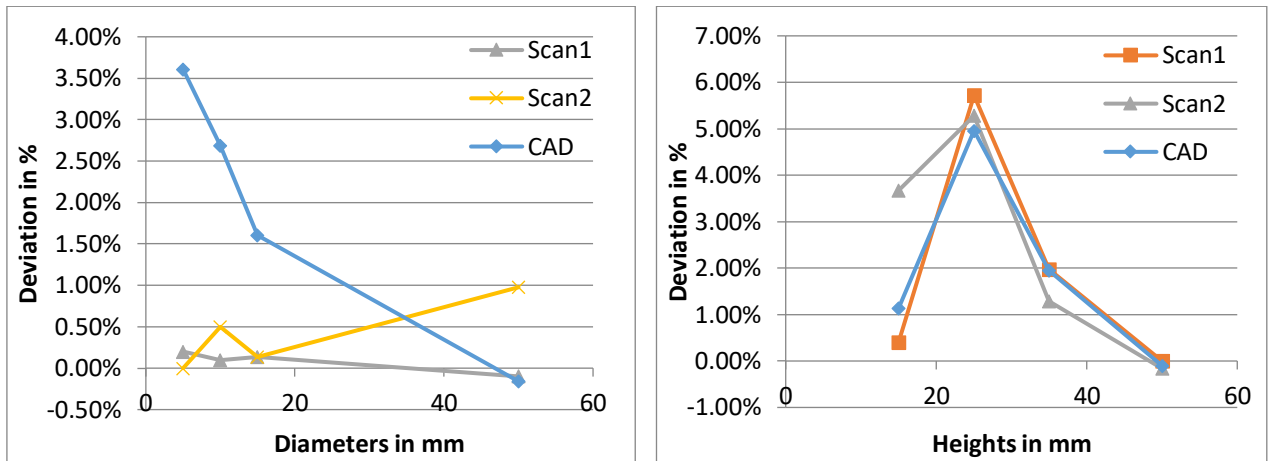


Figure 4.25. Plots of measurements v/s deviation of sample2

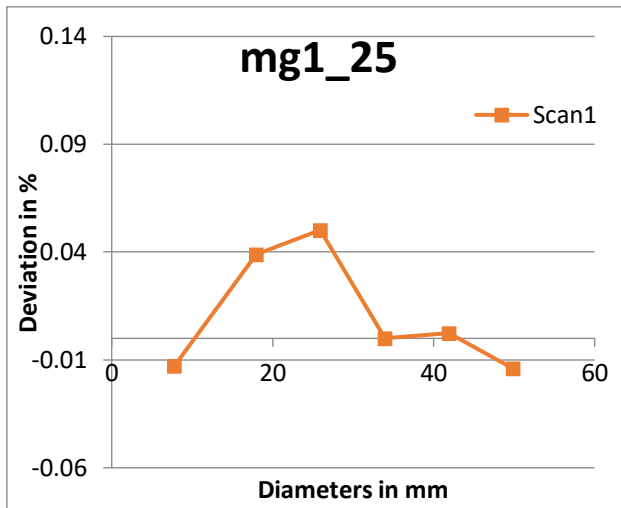
The dimensions of the plexiglass step cylinder (sample3) are measured by fitting different shapes, cylinders for step diameter measurement and planes for step height measurement. Six cylinders were considered one for each step, that is for five steps (1 to 5) and last one (6) for centre hole that runs throughout the cylinder. Six planes were considered, one at the bottom of the cylinder and the rest in the middle of each step. The table (5.6) shows the measurements of different CT data obtained from different parameter sets along with the CMM measurements which were measured using mitutoyo measuring machine containing all the 6 diameters, including the hole diameter, and 6 heights, including the height of the whole cylinder of different. All the measurements are in mm.

Table 4.6. Measurements of step cylinder for different CT scan data

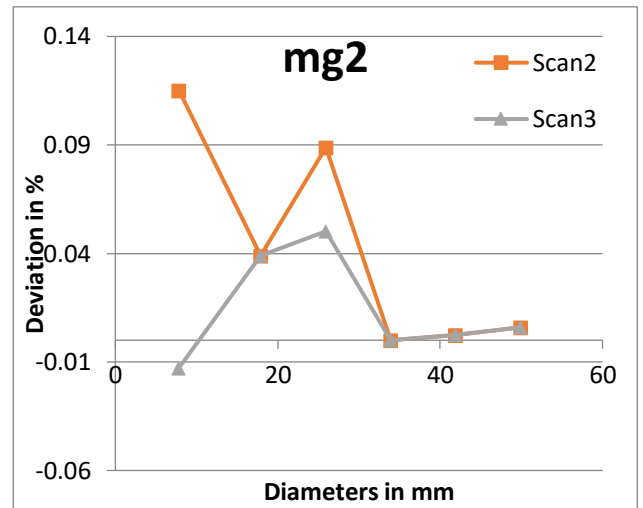
	Diameters						Heights					
	Step1	Step2	Step3	Step4	Step5	Hole6	Step1	Step2	Step 3	Step4	Step5	Cylinder6
CMM measurements	49.87 7	41.879	33.910	25.887	17.923	7.811	-	9.650	10.306	9.931	9.938	-
Scan1	49.87	41.88	33.91	25.90	17.93	7.81	9.18	9.64	10.30	9.96	9.93	48.99
Scan2	49.88	41.88	33.91	25.91	17.93	7.82	9.19	9.64	10.30	9.95	9.93	49.00
Scan3	49.88	41.88	33.91	25.90	17.93	7.81	9.17	9.64	10.30	9.95	9.93	48.98
Scan4	49.87	41.87	33.90	25.90	17.93	7.82	9.05	9.69	10.32	9.95	9.95	48.95
Scan5	49.87	41.87	33.90	25.90	17.93	7.82	9.08	9.64	10.30	9.89	10.04	48.96
Scan6	49.87	41.87	33.90	25.90	17.93	7.81	9.10	9.66	10.31	9.83	10.06	48.96
Scan7	49.87	41.87	33.90	25.90	17.93	7.82	9.08	9.69	10.24	9.97	9.94	48.92
Scan8	49.86	41.86	33.89	25.90	17.92	7.81	9.22	9.65	10.30	9.93	9.92	48.96
Scan9	49.86	41.86	33.89	25.90	17.92	7.81	9.07	9.61	10.36	9.90	10.01	48.93

Scan10	49.85	41.86	33.89	25.90	17.92	7.81	9.00	9.76	10.23	9.91	10.02	48.91
Scan11	49.86	41.86	33.89	25.90	17.92	7.81	9.18	9.64	10.30	9.94	9.95	49.00
Scan12	49.85	41.86	33.89	25.89	17.92	7.81	9.10	9.64	10.32	9.95	9.95	48.94

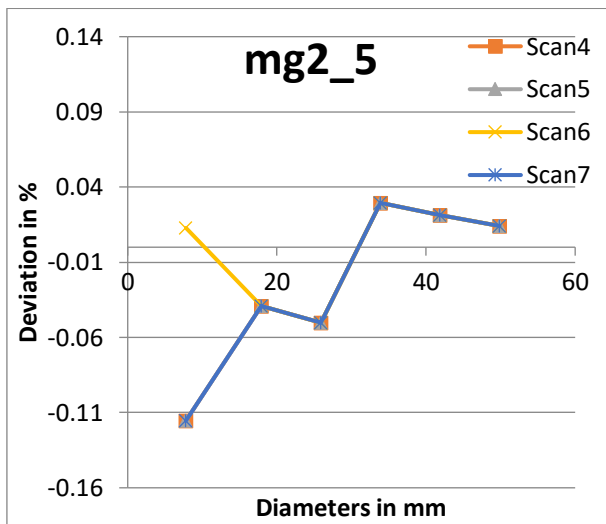
From the table above the measurements compared to one another does not show much difference. But all the measurements have a little deviation which is calculated using equation (4.1). For better understanding these deviations were plotted considering the diameters of each step, according to the same magnification factor as sorted in the table (5.2) of the CT data sets.



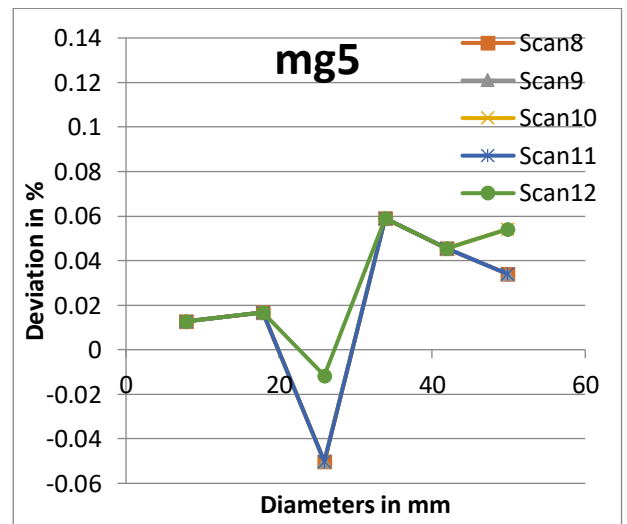
(a)



(b)



(c)



(d)

Figure 4.26. Plots of diameters v/s its deviation of sample3 according to the magnification factor

According to different magnification value the plots are generated for the diameters and its deviation with respect to the CMM diameter measurements which are shown in figure (5.26), the parameter set with least deviation from each of the four figures are noted to finally obtain the optimized parameter set which is best for scanning of sample3,plexiglass step cylinder. The below figure (5.27) shows the deviation plots of the selected parameters sets that is, scan1 with magnification1.25, 100kV voltage, 200uA current, 666ms average time, voxel size of 160 um and a

focus size of 10um; scan3 with magnification2, 200kV voltage, 200uA current, 666ms average time, voxel size of 100um and 42um of focus size; scan6 with magnification2.5, 100kV voltage, 200uA current, 600ms average time, voxel size of 80um and 10um of focus size; and finally scan12 with magnification5, 200kV voltage, 200uA current, 600ms average time, voxel size of 40um and 42um of focus size and CMM measurement deviation curve.

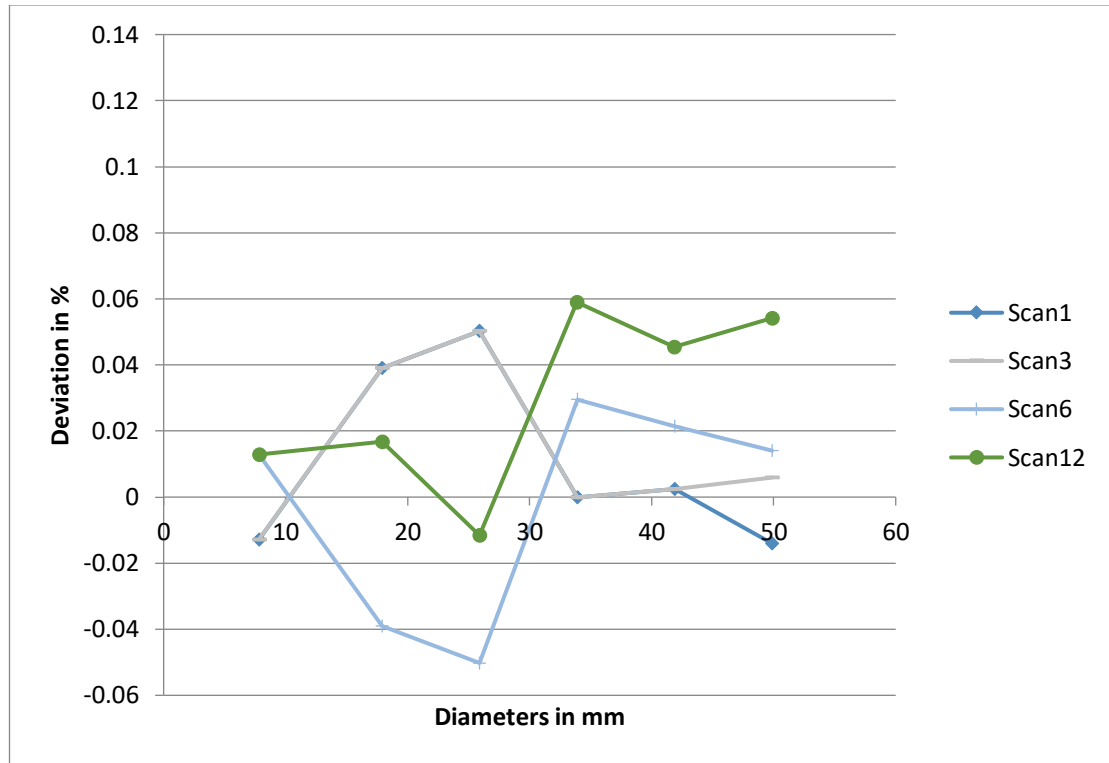


Figure 4.27. Diameter v/s its deviation curves with different magnification value

From the deviation plots the parameter set of scan3 seems to have the least deviation on an average but the quality of CT image of this parameter set is low which conflicts with the measurement result but the deviation of all the parameter sets are negligible scan1 deviations are also very low compared to all others and hence, the parameter set of scan1 in table (5.2) with magnification1.25, 100kV voltage, 200uA current, 666ms average time, voxel size of 160um and 10um of focus size is recommended for CT scan of the plexiglass step cylinder. In the above investigation only diameters are considered, although the overall measurements carried out using CT data does not show much of deviations from the original design measurements shown in figure (5.3). The height of one of the step and the whole cylinder height could not be measured using CMM, this highlights the disadvantage of CMM approach and also the advantage of XCT approach for reverse engineering process.

The hole in the centre of the cylinder runs throughout the cylinder, so there may be variation in its diameter all along hence; its diameter is measured at each step of the step cylinder. The measurements are carried out by considering each step of the cylinder and fitting a cylinder into the hole and measuring its diameter. The diameter of the hole at each step is measured, that is at five steps for five different scanned CT data's, table (5.8) below gives these measurements which are given in mm. There are slight deviations in the diameter of the hole at each step.

Table 4.7. Measurements of the diameter of the hole at each step of step cylinder for different CT data

	Hole diameter at each step for CT data's scanned at different parameters				
	Scan1	Scan2	Scan3	Scan4	Scan5
Step1	7.84	7.84	7.83	7.78	7.84
Step2	7.82	7.82	7.82	7.82	7.82
Step3	7.81	7.81	7.80	7.81	7.81
Step4	7.80	7.80	7.80	7.80	7.80
Step5	7.80	7.81	7.80	7.80	7.81

The diameters of the hole at each step are plotted with respect to the outer step diameter for the different scan parameter sets which is shown in figure (5.28) below. This figure gives a better understanding of how the hole diameter varies along the cylinder length for different scans with different parameter sets.

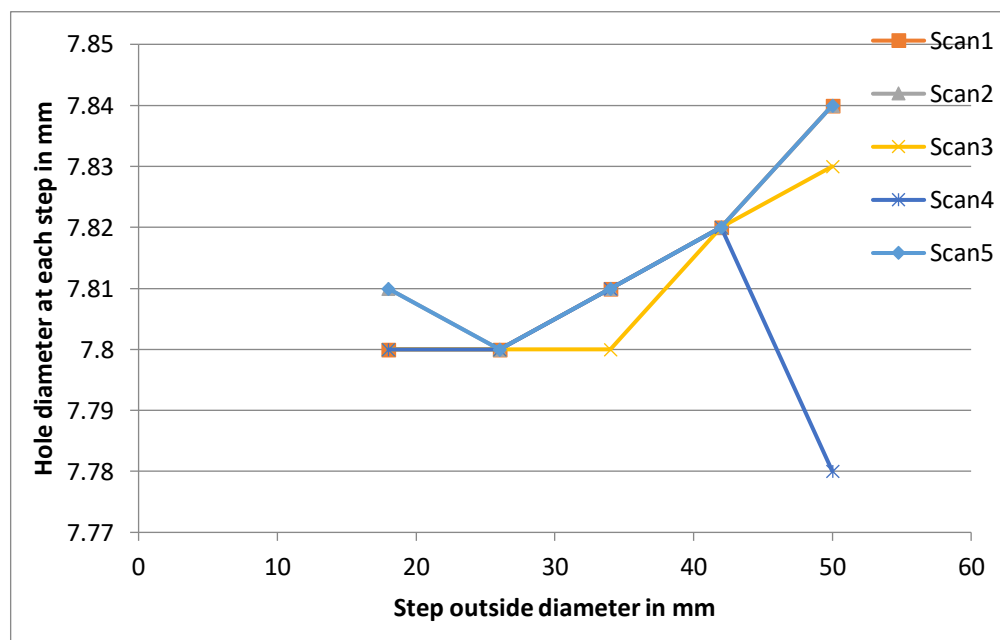


Figure 4.28. Hole diameter at each step with respect to outside step diameters

The CT data of aluminum step cylinder, sample4 were also measured in the same way as that of plexiglass step cylinder. For measuring the sample different shapes were considered like the cylinders for each step for diameter measurement and planes at each step for measuring of each step height. The measurement of the sample for each CT data was tabulated and is presented in the table (5.9) below, which shows the measurements of different scans with different parameter sets and also the CMM measurements which were measured using mitutoyo measuring machine. All measurements are in mm.

Table 4.8. Measurements of the aluminum step cylinder

	Diameters						Heights					
	Step1	Step2	Step3	Step4	Step5	Hole6	Step1	Step2	Step 3	Step4	Step5	Cylinder6
CMM measurements	49.926	41.937	33.932	25.931	17.959	7.897	-	10.234	9.943	10.118	9.697	
Scan1	49.94	41.94	33.95	25.95	17.98	7.86	9.49	10.42	10.19	10.13	9.73	49.24
Scan2	49.94	41.95	33.95	25.95	17.98	7.86	9.15	10.23	9.93	10.06	9.77	49.13
Scan3	49.94	41.96	33.95	25.96	17.98	7.86	9.13	10.23	9.95	10.12	9.69	49.13
Scan4	49.90	41.92	33.92	25.93	17.96	7.86	9.28	10.21	9.96	10.13	9.75	49.29
Scan5	49.90	41.91	33.92	25.93	17.96	7.86	9.27	10.22	9.96	10.15	9.73	49.27
Scan6	49.91	41.92	33.93	25.93	17.96	7.87	9.16	10.23	9.91	10.14	9.70	49.14

Similar to the plexiglass step cylinder, from the table above the measurements of aluminium, compared to one another does not show much difference. But all the measurements have a little deviation from the original design of the step cylinder. For better understanding these deviations were also plotted considering the diameters of each step, according to the same magnification factor as sorted in the table (5.3).

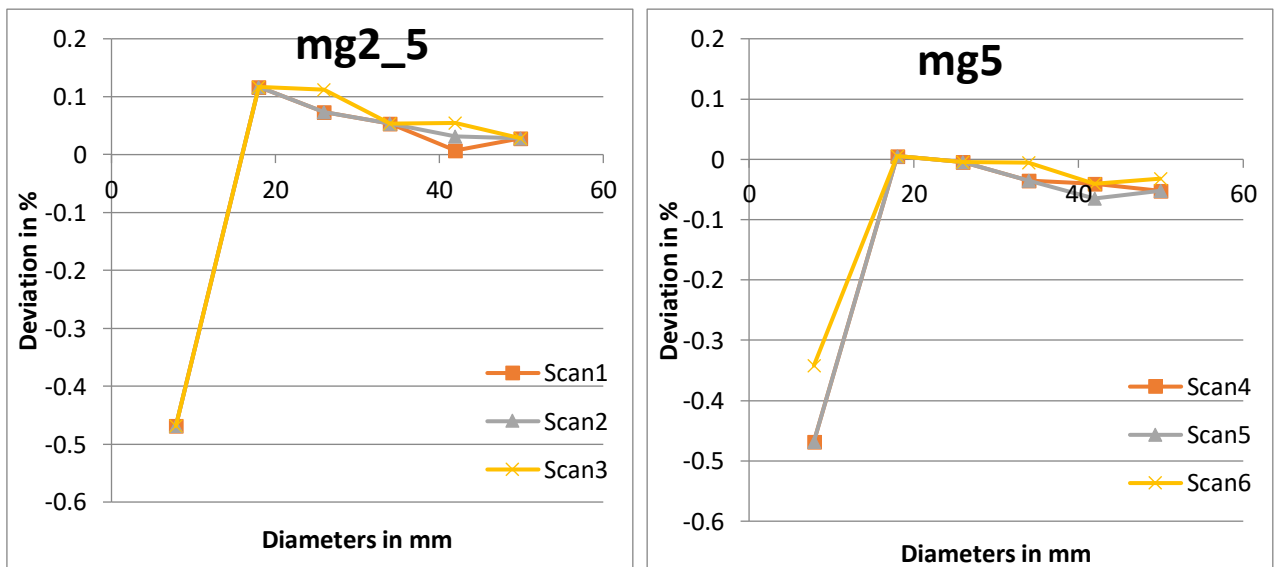


Figure 4.29. Plots of diameters v/s its deviation of sample4 according to the magnification factor

According to different magnification value, magnification2.5 and 5, the plots are generated for the diameters which are shown in figure (5.29), the parameter set with least deviation from each of the two figures are noted to finally obtain the optimized parameter set which is best for scanning of aluminium step cylinder (sample4). The below figure (5.30) shows the deviation plots of the selected parameters set, that is, scan1 with magnification2.5, 200kV voltage, 200uA current,

1000ms average time, voxel size of 80um and 10um of focus size and scan6 with magnification5, 100kV voltage, 200uA current, 2000ms average time, voxel size of 40um and 10um of focus size.

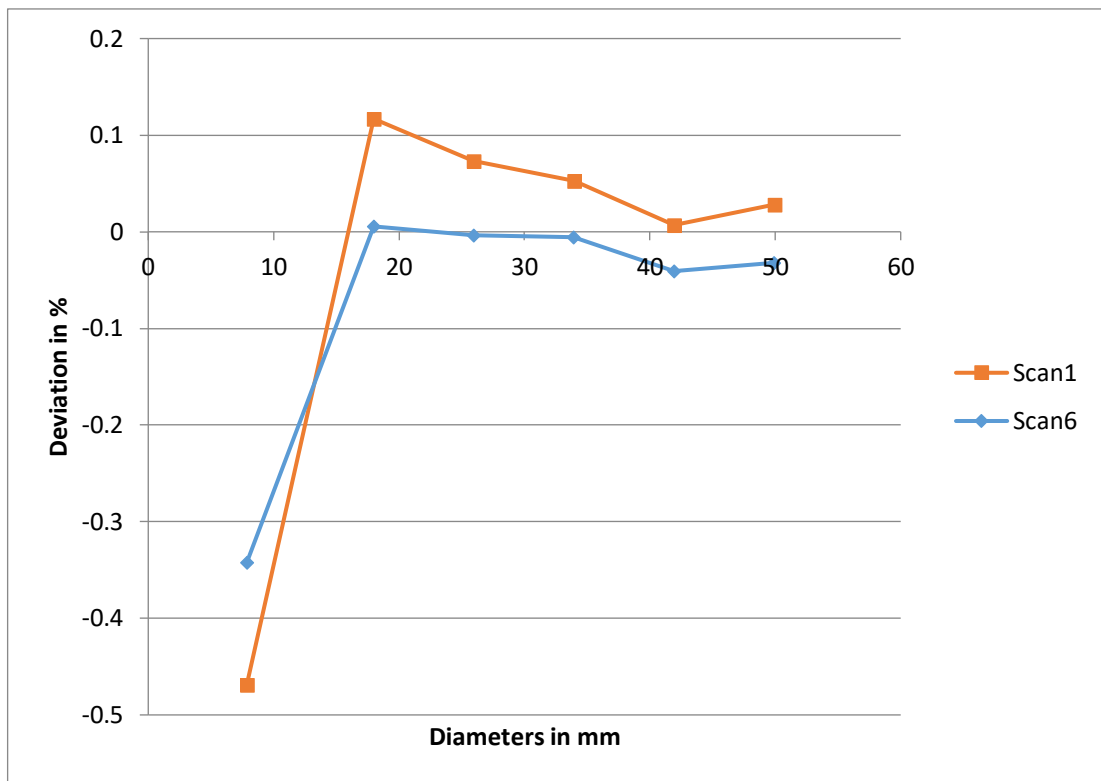


Figure 4.30. Diameter v/s its deviation curves with different magnification value

Considering the above plots in figure (5.30), the plot with least deviation is the scan6 parameter set with magnification5, 100kV voltage, 200uA current, 2000ms average time, voxel size of 40um and 10um of focus size. Hence, the parameter set of scan6 with the mentioned parameters is recommended for CT scanning of aluminum step cylinder. In the above investigation only diameters are considered although the overall measurements carried out using CT data does not show much of deviations from the original design measurements shown in figure (5.3). The height of one of the step and the whole cylinder height could not be measured using CMM, this highlights the disadvantage of CMM approach and also the advantage of XCT approach for reverse engineering process.

All the measurements considered in this experiment for different shapes and different material samples have very low deviation or errors which are seen in this section. Thus measurement accuracy is very high, that is 98% - 99% which increases the overall accuracy of the reverse engineering process using X-ray computed tomography. Even with the different parameter scan the variation in the measurements compared to the original measurements are very low.

4.6. Mesh conversion

Converting the processed and analyzed CT data (images) to a mesh file was carried out to complete the reverse engineering process. Different iterations were carried out to find the optimum mesh conversion parameters. Different iterations, time taken for the completion of the process and the respective surface determination parameter are shown in the table (5.10) below.

Table 4.9. Iterations of Mesh conversion process

Type of mesh	Surface determination	Duration of process
Ray based	Remove noise particles	5 hours 45 min
	Remove particles and all voids	6 hours 15 min
	Remove particles and all voids	8 hours
	Manual and remove noise particles	Aborted due to long duration
	Remove particles and all voids	4 hours
	Manual and remove noise particles	less than a minute

After surface determination and measuring of the samples these samples are then meshed to carry out the next step that is conversion to 3D CAD model. Figure (5.31) shows the meshed images of sample1 of the scan1 parameter set of table (5.1). Even in these samples the artifacts are visible as in the CT images which are highlighted, this hinders the process and makes it time consuming.

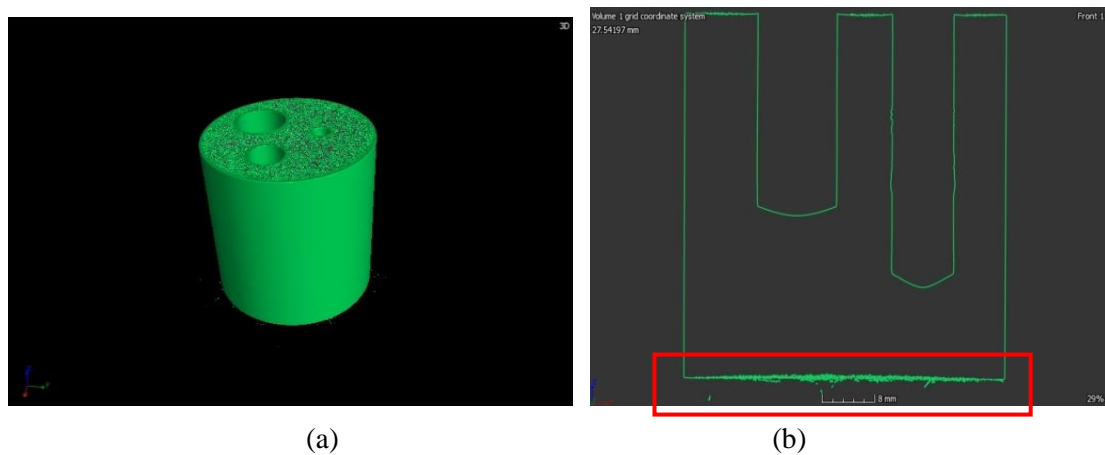


Figure 4.31. Meshed images of scan1 parameter set of sample2. (a) 3D view (b) Front view (c) Right view

The measurement results compared to each other does not show much difference from the two different scans but other processes and analysis prove that the scan2 parameter set gives better results compared to scan1 data. The meshed images of these CT images without artifacts are shown in figure (5.32). This way in each step the accuracy of results obtained after each process is analyzed along with the sources that hinder the accuracy. Many iteration were carried out and the best result with high accurate result is recommended, that is the scan2 parameter set is recommended.

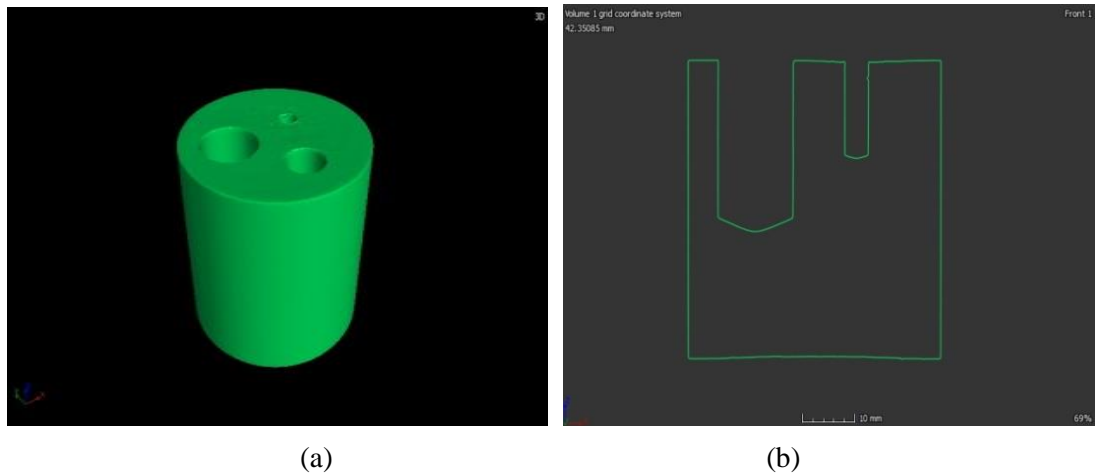


Figure 4.32. Meshed images of scan2 parameter set of sample2. (a) 3D view (b) Right view

For sample3 as well with all the scanned data, the CT data was converted to mesh using the parameters mentioned in the previous section. This mesh converted file was also free from noise as that of the CT images which are shown in below images of figure (5.33), which has a proper surface which is shown in 2D (left image). The file size was small enough (6.5 Mb) that it could be easily imported in solidworks software to get the CAD file.

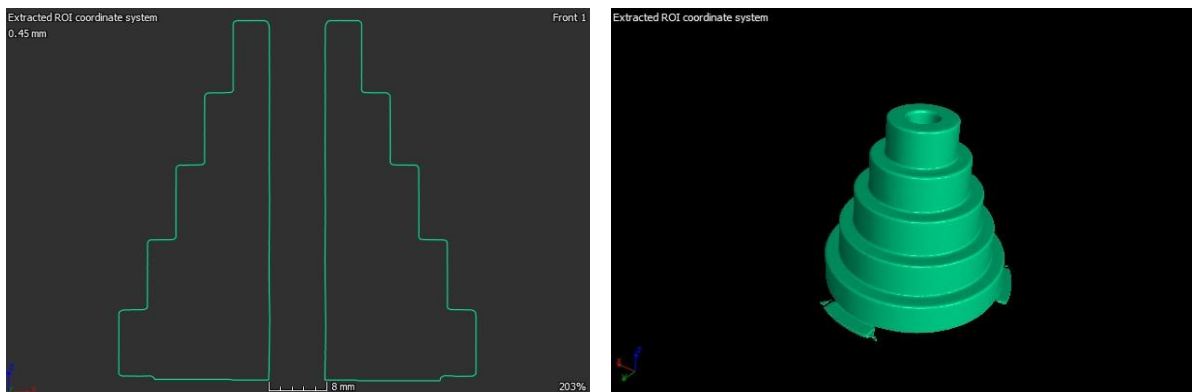


Figure 4.33. Meshed CT images of step cylinder of plexiglass step cylinder

For the parameter set of scan8, the usual procedure for the mesh conversion was carried out, but the mesh created was a hallow one. The first iteration of mesh conversion was failed as the mesh did not form a closed surface at the bottom of the sample as in figure (5.34a) resulting in a hollow step cylindrical mesh which is shown in figure (5.34b).

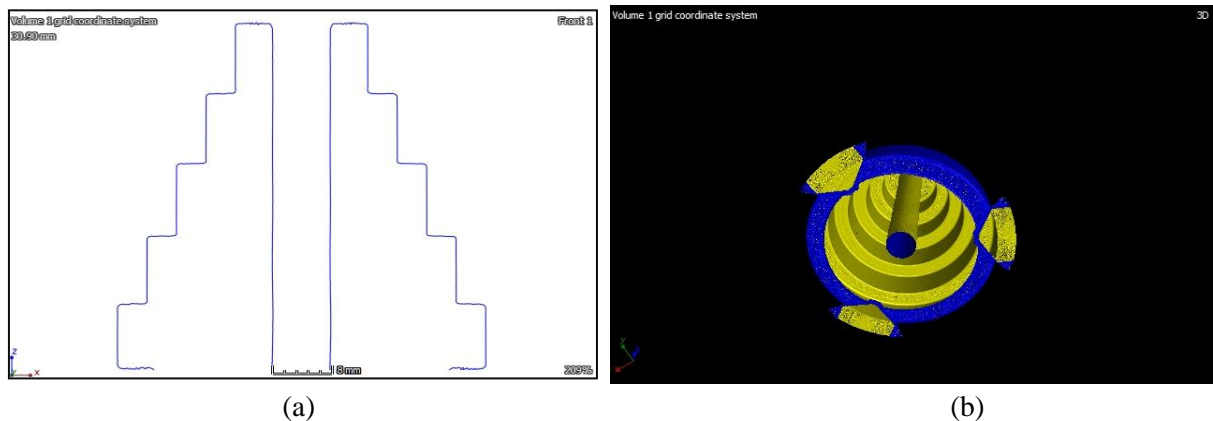


Figure 4.34. Improperly meshed CT images of step cylinder of scan8 parameter set of plexiglass step cylinder

The process was repeated with same parameters except for the consideration of surface determination, where a gray value of 20,000 was set. The meshed CT images are shown in figure (5.35) below. The file size of the mesh file is small (33 Mb) which can be imported in Solidworks software to get the CAD file.



Figure 4.35. Meshed CT images of scan8 parameter set of plexiglass step cylinder

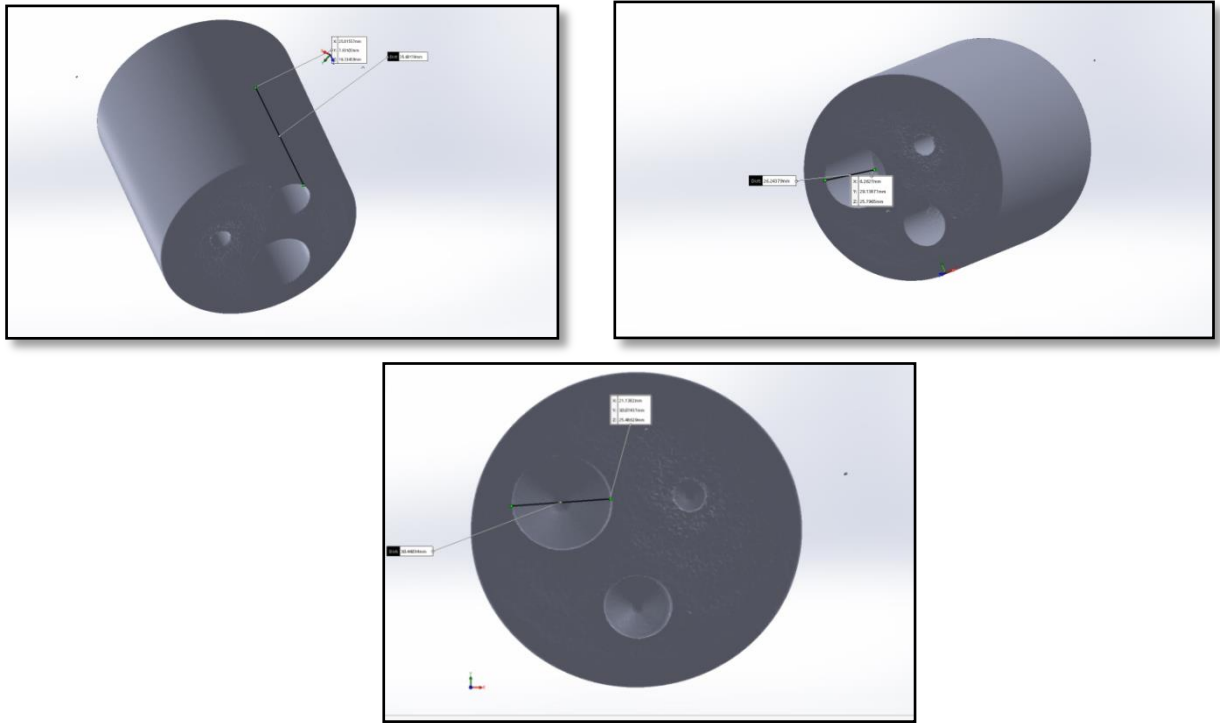
The mesh conversion procedure was carried out in the same way for the aluminum step cylinder as well. These mesh images also were free from noise as the CT images which helped in fast conversion giving the high accuracy rate for the overall process. The figure (5.36) below shows the mesh images of the aluminum step cylinder.



Figure 4.36. Meshed CT images of step cylinder of aluminum step cylinder

4.7. Conversion of 3D CAD model

After the first three steps, the final step to complete the process of reverse engineering is the 3D CAD modeling. When the mesh files are obtained from the VGStudio max software, the mesh files, which are in .stl format, are imported into the solidworks software to obtain the final CAD model. After each process, the result is analyzed for the accuracy and the sources of the uncertainties that affect them. The final CAD model was compared with the original CAD design to check the final accuracy. Only sample2 is considered and the CAD images are shown in figure (5.37) below which is the final product of the scan2 parameter set as CT data of scan1 was not able to complete the process of reverse engineering as it was not possible to import it in the solidworks software as the mesh file was too large. These 3D CAD models are then compared with the initially designed CAD models and the accuracy is assessed which is given in table (5.5).



(c)

Figure 4.37. Mesh file converted to CAD file

Conclusion

The accuracy of reverse engineering is affected from the initial process that is the data acquisition using computed tomography. The first source of uncertainty is the x-ray parameters like the voltage, current, voxel size, magnification etc. The distance between the source and the object is also one of the sources of uncertainty. Here we use cone beam x-ray scan, hence if the object is placed close to the source the possibilities of artifacts in the CT images are higher. In the analysis of cylinder with cylindrical defects or holes (sample2), because of incorrect positioning the processes like surface determination and mesh conversion would take 2 hours and 2 days respectively but with correct positioning it takes only 10min and less than a minute. After correcting the parameters of x-ray scan the CT images obtained were free from artifacts which were visually proven by the CT images. Hence for the sample1 and sample2 the scan2 parameter set with 110kV voltage, 200uA current, 22 watts power, focus size of 31 um, voxel size of 32.19 um and with a distance of 244.11mm from source to object is recommended.

A step cylinder sample was considered for deeper investigation of the accuracy which was produced from plexiglass and aluminum. The measurement deviations of plexiglass step cylinder the parameter set of scan1 with magnification1.25, 100kV voltage, 200uA current, 666ms average time, voxel size of 160um and 10um of focus size has the least deviation on an average compared to others and hence, this parameter set is recommended for CT scan of the plexiglass step cylinder. The CT data with this parameter set has good gray value distribution curve as well, which gives the better accuracy compared to other parameter sets which matches with the measurement results.

Considering the measurement deviations of aluminum step cylinder sample (sample4) the plot with least deviation is the scan6 parameter set with magnification5, 100kV voltage, 200uA current, 2000ms average time, voxel size of 40um and 10um of focus size. Hence, the data with this parameter set is recommended for CT scanning of aluminum step cylinder. This CT data with parameter set has good gray value distribution curve as well, which gives the better accuracy compared to other parameter sets which matches with the measurement results. Even the distribution curves plotted at different step also gave almost flat surfaces indication the good quality of the CT data.

From the overall experiment, the results of the measurement analysis were almost 99% accurate and the gray scale analysis also gave flat curves indicating the absence of noise. This makes the overall accuracy of the x-ray computed tomography approach for the process of reverse engineering to be 98-99% on an average. The CMM approach could not give all the required measurements which indicate that the reverse engineering process through the CMM approach is not successful for the samples considered. Hence the X-ray computed tomography approach is advantageous and is recommended for the purpose of reverse engineering than the CMM approach.

References

- [1] M. H. M, S. R. Ch, and K. E. Prasad, "REVERSE ENGINEERING : POINT CLOUD GENERATION WITH CMM FOR PART MODELING AND ERROR ANALYSIS," vol. 3, no. 4, pp. 2006–2009, 2008.
- [2] J. Noel and N. Star, "Advantages of CT in 3D Scanning of Industrial Parts," vol. 1, no. 3, 2008.
- [3] S. E. Quadir *et al.*, "A Survey on Chip to System Reverse Engineering," *ACM J. Emerg. Technol. Comput. Syst.*, vol. 13, no. 1, pp. 1–34, 2016.
- [4] F. Buonamici, M. Carfagni, R. Furferi, L. Governi, A. Lapini, and Y. Volpe, "Journal of Computational Design and Engineering Reverse engineering of mechanical parts: A template-based approach," *J. Comput. Des. Eng.*, vol. 5, no. 2, pp. 145–159, 2018.
- [5] N. Anwer and L. Mathieu, "CIRP Annals - Manufacturing Technology From reverse engineering to shape engineering in mechanical design," *CIRP Ann. - Manuf. Technol.*, vol. 65, no. 1, pp. 165–168, 2016.
- [6] "<https://www.machinedesign.com/3d-printing-cad/article/21837371/whats-the-difference-between-ct-and-cmm>"
- [7] K. Schröder, A. Zinke, and R. Klein, "Image-based reverse engineering and visual prototyping of woven cloth," *IEEE Trans. Vis. Comput. Graph.*, vol. 21, no. 2, pp. 188–200, 2015.
- [8] R. Che, S. Azmi, and R. Daud, "Morphological Operation on Printed Circuit Board Reverse Engineering using MATLAB," pp. 529–533, 2006.
- [9] S. Gholizadeh, "ScienceDirect ScienceDirect ScienceDirect A review review of of non-destructive non-destructive testing testing methods methods of of composite composite materials materials Thermo-mechanical of a high pressure turbine blade of an airplane gas turbine engine," *Procedia Struct. Integr.*, vol. 1, pp. 50–57, 2016.
- [10] L. Li, C. Li, Y. Tang, and Y. Du, "Robotics and Computer – Integrated Manufacturing An integrated approach of reverse engineering aided remanufacturing process for worn components," *Robot. Comput. Integr. Manuf.*, vol. 48, no. November 2015, pp. 39–50, 2017.
- [11] K. Sokó and D. Cekus, "Reverse engineering as a solution in parts restoration process," *Procedia Eng.*, vol. 177, pp. 210–217, 2017.
- [12] K. M. M. H. S. A. Abdullah, "Reverse engineering of turbine blades based on design intent," pp. 1009–1020, 2007.
- [13] I. Kovács, T. Várady, and P. Salvi, "Applying geometric constraints for perfecting CAD models in reverse engineering," vol. 82, pp. 44–57, 2015.
- [14] W. Sun, S. Brown, P. Woolliams, and M. M. Attallah, "Applications and systematic errors of X-ray computed tomography associated with dimensional metrology," no. December, 2016.
- [15] V. Aloisi, S. Carmignato, J. Schlecht, and E. Ferley, "Investigation on the effects of X-ray CT system geometrical misalignments on dimensional measurement errors," no. iCT, pp. 1–6, 2017.
- [16] M. Reiter, D. Weiß, C. Gusenbauer, M. Erler, C. Kuhn, and J. Kastner, "Evaluation of a histogram-based image quality measure for X-ray computed tomography," pp. 273–282.
- [17] A. Townsend, A. Townsend, L. Pagani, P. Scott, and L. Blunt, "Areal surface texture data extraction from X-ray computed tomography reconstructions of metal additively manufactured parts Areal surface texture data extraction from X-ray computed tomography reconstructions of metal additively manufactured parts," *Precis. Eng.*, vol. 48, no. December,

- pp. 254–264, 2016.
- [18] “VGSTUDIO MAX Reference Manual”
 - [19] T. Report and E. Bj, “Gray Scale Image Analysis : Image analysis program for use with MATLAB Gray Scale Image Analysis 2006 Image analysis program for use with MATLAB Physics of Geological Processes Department of Physics University of Oslo,” no. March, 2015.
 - [20] M. Reiter *et al.*, “Evaluation of transmission based image quality optimisation for X-ray computed tomography,” pp. 241–250.
 - [21] “STUDY ON PARAMETER VARIATION OF AN INDUSTRIAL COMPUTED TOMOGRAPHY SIMULATION TOOL CONCERNING DIMENSIONAL MEASUREMENT DEVIATIONS Michael REITER.”
 - [22] M. Reiter, B. Harrer, C. Heinzl, and D. Salaberger, “Simulation Aided Study for Optimising Industrial X-ray CT Scan Parameters for Non-Destructive Testing and Materials Characterisation,” pp. 1–9.

Appendices

Appendix 1. The International Young Scientists Conference “Industrial Engineering 2019” on topic “Assessment of Factors Influencing Accuracy in a Computed Tomography based Reverse Engineering”.